Cytological and Transcriptomic Analyses Reveal Important Roles of *CLE19* in Pollen Exine Formation[1][OPEN]

Shuangshuang Wang,[a] Jianan Lu,[a] Xiu-Fen Song,[b] Shi-Chao Ren,[b] Chenjiang You,[a] Jie Xu,[c] Chun-Ming Liu,[b,d] Hong Ma,[a] and Fang Chang[a,2]

[a]State Key Laboratory of Genetic Engineering and Collaborative Innovation Center for Genetics and Development, Ministry of Education Key Laboratory of Biodiversity Sciences and Ecological Engineering and Institute of Biodiversity Sciences, Institute of Plant Biology, School of Life Sciences, Fudan University, Shanghai 200438, China

[b]Key Laboratory of Plant Molecular Physiology, Institute of Botany, Chinese Academy of Sciences, Beijing 100093, China

[c]Collaborative Innovation Center for Genetics and Development, School of Life Sciences and Biotechnology, Shanghai Jiao Tong University, Shanghai 200240, China

[d]Institute of Crop Science, Chinese Academy of Agricultural Science, Beijing 100081, China

ORCID IDs: 0000-0001-5293-3302 (S.W.); 0000-0002-7271-362X (C.-M.L.); 0000-0001-8717-4422 (H.M.); 0000-0003-3378-8829 (F.C.).

The CLAVATA3/ESR-RELATED (CLE) peptide signals are required for cell-cell communication in several plant growth and developmental processes. However, little is known regarding the possible functions of the CLEs in the anther. Here, we show that a T-DNA insertional mutant, and dominant-negative (DN) and overexpression (OX) transgenic plants of the *CLE19* gene, exhibited significantly reduced anther size and pollen grain number and abnormal pollen wall formation in Arabidopsis (*Arabidopsis thaliana*). Interestingly, the *DN-CLE19* pollen grains showed a more extensively covered surface, but *CLE19-OX* pollen exine exhibited clearly missing connections in the network and lacked separation between areas that normally form the lacunae. With a combination of cell biological, genetic, and transcriptomic analyses on *cle19*, *DN-CLE19*, and *CLE19-OX* plants, we demonstrated that *CLE19-OX* plants produced highly vacuolated and swollen *aborted microspores* (*ams*)-like tapetal cells, lacked lipidic tapetosomes and elaioplasts, and had abnormal pollen primexine without obvious accumulation of sporopollenin precursors. Moreover, *CLE19* is important for the normal expression of more than 1,000 genes, including the transcription factor gene *AMS*, 280 *AMS*-downstream genes, and other genes involved in pollen coat and pollen exine formation, lipid metabolism, pollen germination, and hormone metabolism. In addition, the *DN-CLE19(+/+) ams(−/−)* plants exhibited the *ams* anther phenotype and *ams(+/−)* partially suppressed the *DN-CLE19* transgene-induced pollen exine defects. These findings demonstrate that the proper amount of CLE19 signal is essential for the normal expression of *AMS* and its downstream gene networks in the regulation of anther development and pollen exine formation.

Pollen grains are generated in the male reproductive organ anther of flowering plants and are essential for plant fertility. In the model plant Arabidopsis (*Arabidopsis thaliana*), pollen grains are ellipsoidal, and the pollen surface is covered by a reticulate exine. In contrast, rice (*Oryza sativa*) pollen grains are globular and have a smooth surface without the reticulate structure. A well-organized pollen wall structure is essential for the physical and chemical stability of the mature pollen by providing protection for pollen grains from environmental stresses, such as desiccation and microbial attacks (Scott et al., 2004). The pollen wall is composed mainly of three layers: the intine layer, the exine layer, and the pollen coat (Zinkl et al., 1999; Edlund et al., 2004; Blackmore et al., 2007). The intine is the innermost layer of the pollen wall immediately adjacent to the plasma membrane of the pollen vegetative cell and is composed mainly of pectin, cellulose, hemicellulose, hydrolytic enzymes, and hydrophobic proteins (Scott et al., 2004). Both the exine layer and the pollen coat layer are basically of a lipidic nature. The exine is largely formed from acyl lipid and phenylpropanoid precursors, which together form the mixed stable biopolymer known as sporopollenin (Guilford et al., 1988; Bedinger et al., 1994; Thom et al., 1998). The pollen exine has many important functions in the prevention of dehydration of male gametophytes, the facilitation of pollen dispersal, and

[1] This work was supported by grants from the National Natural Science Foundation of China (31130006, 31470282, 31670316, and 31370029) and the State Key Laboratory of Genetic Engineering at Fudan University.

[2] Address correspondence to fangchang@fudan.edu.cn.

The author responsible for distribution of materials integral to the findings presented in this article in accordance with the policy described in the Instructions for Authors (www.plantphysiol.org) is: Fang Chang (fangchang@fudan.edu.cn).

S.W., H.M., and F.C. designed the research; S.W. performed the RNA in situ hybridization analysis, the phenotypic observation, the real-time PCR experiments, the scanning electron microscopy and transmission electron microscopy observations, and tissue collection for the transcriptome; S.-C.R., X.-F.S., and C.-M.L. generated the *DN-CLE* transgenic mutants; J.L. and C.Y. together carried out the transcriptome analysis; S.W. and F.C. analyzed the data and wrote the article; F.C. and H.M. revised the manuscript.

[OPEN] Articles can be viewed without a subscription.

www.plantphysiol.org/cgi/doi/10.1104/pp.17.00439

pollen-stigma recognition and adhesion (Zinkl et al., 1999). The pollen coat fills the cavities of the pollen exine during the late stages of pollen development, and previous studies have demonstrated that developmental defects of pollen wall structure or lack of pollen coat lipids in Arabidopsis lead to a failure or delay of pollen hydration and subsequent male sterility (Preuss et al., 1993; Mayfield and Preuss, 2000; Wilson and Zhang, 2009; Li and Zhang, 2010).

Anther development is precisely regulated temporally by transcriptional networks, receptor-like protein kinase-mediated signal pathways, and other pathways (Ma, 2005; Ge et al., 2010; Chang et al., 2011). The basic helix-loop-helix (bHLH) transcriptional factor DYSFUNCTIONAL TAPETUM1 (DYT1) is among the earliest acting male-specific regulators and is required for the normal development of tapetum by regulating the normal expression of more than 1,000 anther genes, and *dyt1* mutants form abnormal prematurely vacuolated tapetal cells and lack mature pollen (Zhang et al., 2006; Feng et al., 2012; Gu et al., 2014; Zhu et al., 2015). In addition, bHLH010, bHLH089, and bHLH091 together are required for normal tapetum development and transcriptome and pollen fertility, forming both feed-forward and feedback loops with DYT1 (Zhu et al., 2015; Cui et al., 2016). Another bHLH transcription factor, ABORTED MICROSPORES (AMS), is a key regulator of anther transcriptome, sporopollenin biosynthesis and secretion, and pollen wall formation (Sorensen et al., 2003; Xu et al., 2010; Feng et al., 2012; Ma et al., 2012; Xu et al., 2014). *DEFECTIVE IN TAPETAL DEVELOPMENT AND FUNCTION* (*TDF1*)/*MYB35* encodes a putative R2R3 MYB transcription factor, and loss of *TDF1* function due to mutation or transgene causes tapetal hypertrophy extending into the locule and results in sporophytic male sterility (Zhu et al., 2008; Feng et al., 2012). MALE STERILITY1 (MS1) is a PHD-finger motif-containing nuclear protein and is essential for tapetum development at the postmeiotic phase and regulates genes important for exine formation (Wilson et al., 2001; Ito et al., 2007). In addition, another R2R3 MYB gene, *MS188/MYB103/MYB80*, is required for sporopollenin biosynthesis and sexine formation (Phan et al., 2011; Xiong et al., 2016). Further molecular genetic and bioinformatics studies revealed that these transcription factors likely form a genetic pathway as follows: DYT1, MYB35/TDF1, AMS, MS188/MYB103/MYB80, MS1, and MYB99 from upstream to downstream during anther/pollen development (Ito et al., 2007; Feng et al., 2012).

Extracellular ligands and their receptor-like protein kinase (RLK)-mediated signaling pathways play important roles in the regulation of anther development. In particular, the RLKs EMS1/EXS and SERK1/2 and the secreted peptide TPD1 are required for tapetum formation and function (Canales et al., 2002; Zhao et al., 2002; Yang et al., 2003; Albrecht et al., 2005; Colcombet et al., 2005). Furthermore, the TPD1 protein from microsporocyte precursors/microsporocyte interacts with the Leu-rich repeat domain of the RLK EMS1/EXS expressed in the tapetal precursor/tapetal cells to promote the phosphorylation of EMS1, thereby regulating anther tapetum development and function (Canales et al., 2002; Zhao et al., 2002; Yang et al., 2003, 2005; Jia et al., 2008; Huang et al., 2016; Li et al., 2017). In addition, brassinosteroids and the brassinosteroid cell surface receptor BRASSINOSTEROID INSENSITIVE1 are required for pollen exine formation and pollen release through the regulation of key genes in tapetum and pollen development, such as *AMS*, *MYB103*, *MS1*, and *MS2* (Ye et al., 2010). In addition, several other RLKs are required for normal anther development, but their ligands remain unknown. For instance, ERECTA, ERECTA-LIKE1 (ERL1), and ERL2 are important for anther lobe formation and normal cell patterning (Torii et al., 1996; Shpak et al., 2003; Hord et al., 2008). BARELY ANY MERISTEM1 (BAM1) and BAM2 regulate the formation of anther somatic cell layers, and the *bam1 bam2* double mutant anther forms many pollen mother-like cells but lacks the three subepidermal somatic cell layers (DeYoung et al., 2006; Hord et al., 2006). RECEPTOR-LIKE PROTEIN KINASE2 is essential for the formation of both the tapetum and the middle layer (Mizuno et al., 2007). On the other hand, besides TPD1, no other peptide signals have been implicated in anther or pollen development.

CLAVATA3 (*CLV3*)/*EMBRYO SURROUNDING REGION* (*ESR*)-*RELATED* (*CLE*) genes encode a family of putative peptide ligands, with at least 32 *CLE* members in Arabidopsis (Cock and McCormick, 2001). Mature CLE peptide signals are 12 to 14 amino acids long, and many of them play important roles in various plant developmental processes. For instance, CLV3 is necessary to restrict stem cell numbers in the shoot apical meristem (Fletcher et al., 1999) by promoting the formation of the CLV1/CLV2 protein complex to inhibit the expression of *WUSCHEL* in the organizing center of the shoot apical meristem (Laux et al., 1996; Fiers et al., 2004). CLE8 regulates the size of embryos and seeds and is expressed in the endosperm and the early embryo to promote *WOX8* expression (Fiume and Fletcher, 2012). CLE40 regulates the activity of the root apical meristem and is expressed in differentiating cells in roots and likely acts through the receptor-like kinase CRINKLY4 to restrict the expression and position of *WOX5* (Stahl and Simon, 2009). The CLE19 peptide triggers root meristem consumption in a CLV2-dependent manner (Casamitjana-Martínez et al., 2003; Fiers et al., 2005; Al-Refu et al., 2009). However, whether the *CLE* genes are required for normal anther development still remains unknown.

One difficulty in studying the endogenous functions of these small *CLE* genes is the shortage of genetic materials, namely the mutant plants. In addition, previous studies revealed that T-DNA insertion mutants of *CLE1*, *CLE7*, *CLE10*, *CLE16*, *CLE18*, or *CLE19* in Arabidopsis exhibited no visible abnormal phenotype (Fiers et al., 2004; Jun et al., 2010), but overexpression of the *CLE* genes *CLE2*, *CLE3*, *CLE4*, *CLE5*, *CLE6*, *CLE7*, *CLE10*, *CLE11*, and *CLE13* resulted in pleiotropic phenotypes similar to those

of CLV3 or CLE40 overexpression plants, and in vitro application or overexpression of one of the *CLE* genes *CLE19*, *CLE21*, *CLE25*, *CLE42*, and *CLE44* caused similar dwarf and short-root phenotypes (Fiers et al., 2004, 2005; Strabala et al., 2006), suggesting a high level of functional redundancy or overlap among *CLE* members. Fortunately, an antagonistic peptide technology (Song et al., 2013) was developed recently as an effective tool to investigate the endogenous functions of these functionally redundant secreted peptides. Using CLV3 as a test case, Song et al. (2013) examined the antagonistic peptide technology by transformations of wild-type Arabidopsis with constructs carrying the full-length CLV3 with every residue in the peptide-coding region replaced one at a time by Ala to probe the effectiveness of each mutation. They found that the Gly-to-Ala substitution in the core CLE motif caused a dominant-negative (DN) *clv3-2*-like phenotype. Further substitutions of the Gly residue individually with the other 18 possible proteinaceous amino acids determined that the Gly-to-Thr substitution resulted in the strongest antagonistic effect in the wild type (Song et al., 2012, 2013). With this strategy, the peptide signal CLE19 was revealed to be important for cotyledon establishment in embryos and endosperm development (Xu et al., 2015).

Here, we tested *CLE* genes for expression in the anther and show that *CLE9*, *CLE16*, *CLE17*, *CLE19*, *CLE41*, *CLE42*, and *CLE45* were preferentially expressed in tapetal and reproductive cells in the anther. Using the antagonistic peptide technology, we generated DN mutants for these seven genes, and our analyses of these mutant transgenic plants indicated that they are important for normal pollen development, especially for the development of pollen exine. Using *CLE19* as a representative, we further characterized its function in the regulation of pollen exine formation using a combination of morphological molecular and transcriptomic analyses of *cle19*, *DN-CLE19*, and *CLE19-OX* mutants. We finally revealed that *CLE19* acts as a negative regulatory element in tapetum development, sporopollenin biosynthesis, and exine formation, likely through the regulation of the transcription factor AMS and downstream genes. Thus, we propose a novel signaling pathway starting from an extracellular peptide signal and eventually affecting the intracellular transcriptional network that is crucial for the regulation of pollen wall development.

RESULTS

Seven *CLE* Genes Are Expressed Preferentially in Arabidopsis Tapetal and Reproductive Cells

The expression of *CLE* genes in Arabidopsis was first examined by searching public microarray databases (http://bar.utoronto.ca/efp/cgi-bin/efpWeb.cgi and http://www.arabidopsis.org/portals/expression/microarray/ATGenExpress.jsp) and using quantitative real-time PCR and RNA in situ hybridization analyses to detect the expression of these *CLE* genes in the developing anther. Among the 14 *CLE* genes that were included in the microarray expression databases, *CLE9*, *CLE10*, *CLE21*, *CLE26*, *CLE40*, *CLE44*, and *CLV3* exhibited relatively high expression levels in the anther, whereas *CLE6* and *CLE12* were relatively highly expressed in the mature pollen (Supplemental Fig. S1A). Quantitative real-time PCR analyses using Columbia-0 (Col-0) inflorescence and stage 4 to 12 anthers revealed that *CLE9*, *CLE16*, *CLE17*, *CLE25*, *CLE27*, *CLE41*, *CLE42*, and *CLE45* were relatively highly expressed in both inflorescence and stage 4 to 12 anthers (Supplemental Fig. S1B), suggesting that they might be involved in male reproductive development.

Further RNA in situ hybridization analyses were performed to investigate the expression patterns of these anther-expressed *CLE* genes. Strong *CLE9*, *CLE16*, *CLE17*, *CLE19*, *CLE41*, *CLE42*, and *CLE45* signals were detected in the anther at various developmental stages (Fig. 1). For instance, *CLE9* and *CLE16* were both expressed in the tapetum and microspores at anther stages 7 to 10 but not in either cell layer at stage 5 (Fig. 1, A–H). *CLE19* was expressed preferentially in both tapetal and male reproductive cells at anther stages 5 to 7, and *CLE17*, *CLE41*, *CLE42*, and *CLE45* were expressed preferentially in both tapetal and male reproductive cells at anther stages 5 to 10 (Fig. 1, I–AB), suggesting their involvement in regulating tapetum function and pollen development. In addition, their highly similar spatial-temporal expression pattern also suggested that these seven *CLE* genes possibly participate in similar anther developmental processes.

DN Mutant Transgenic Plants of *CLE9*, *CLE16*, *CLE17*, *CLE19*, *CLE41*, *CLE42*, and *CLE45* Exhibited Abnormal Anther Development

To further investigate the functions of the *CLE* genes in anther development, the T-DNA insertional mutants of *CLE9*, *CLE17*, *CLE19*, or *CLE42* and the RNA interference (RNAi) mutant of *CLE16* were obtained (Supplemental Fig. S2), and the transcript levels of these genes in mutant plants were analyzed using real-time quantitative PCR. The *cle9-1*, *cle16-1*, *cle17-1*, *cle19-1* (in the *qrt1-2* background), *cle19-2*, and *cle42-1* mutants exhibited drastically reduced expression of the relevant genes (Supplemental Fig. S2) and were further examined phenotypically. Both *cle19-1 qrt1-2* and *cle19-2* produced abnormally short siliques and had slightly decreased anther size and some aborted pollen grains (Fig. 2, A–E, J–N, S–W, and AB–AF). Considering that *cle19-1* was in the *qrt1-2* background, we observed the phenotypes of silique, flower, anther, and pollen in the *qrt1-2* plants and did not find any defects except for the pollen phenotype (Fig. 2, C, L, U, and AD). The above results suggested that *CLE19* is possibly involved in anther development. In contrast, the *cle9-1*, *cle16-1*, *cle17-1*, and *cle42-1* single mutants all exhibited normal plant growth and flower and anther development (Supplemental Fig. S3; Supplemental Table S1).

Based on the high amino acid similarity between the functional domains of these Arabidopsis CLE members (Ni and Clark, 2006) and the no/weak defects in anther

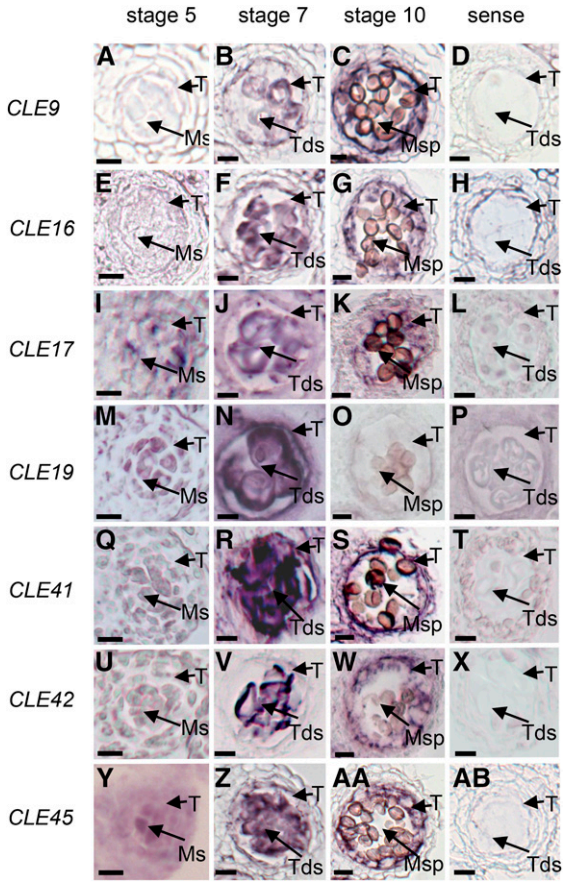

Figure 1. Spatial and temporal expression analyses of *CLE* genes. Expression patterns are shown for *CLE9* (A–D), *CLE16* (E–H), *CLE17* (I–L), *CLE19* (M–P), *CLE41* (Q–T), *CLE42* (U–X), and *CLE45* (Y–AB) in wild-type anthers by RNA in situ hybridization. Sections are from anthers of stage 5 (A, E, I, M, Q, U, and Y), stage 7 (B, F, J, N, R, V, and Z), stage 10 (C, G, K, O, S, W, and AA), and controls (D, H, L, P, T, X, and AB) using sense probe on wild-type stage 7 anthers. Ms, Microsporocytes; Msp, microspores; T, tapetum; Tds, tetrads. Bars = 10 μm.

development observed in the available *cle* single mutants, we proposed a possible functional redundancy among these anther-expressed *CLE* genes in the regulation of anther development. Therefore, we generated double and triple mutants of these *CLE* genes by crossing *cle16-1*, *cle17-1*, *cle19-1*, and *cle42-1*. The *qrt1-2* mutation in *cle19-1* plants segregated away during this process. Compared with the *cle19-1* mutant, our phenotypic and statistical analyses showed that the *cle16 cle19*, *cle17 cle19*, and *cle19 cle42* double mutants had fewer pollen grains in the anther (Supplemental Fig. S4, A–AA; Supplemental Table S1). Moreover, the *cle17 cle19 cle42* triple mutant showed more barren siliques, less pollen amount, and a larger fraction of defective pollen in the anther (Supplemental Fig. S4, A–AA; Supplemental Table S1). In addition, we generated DN mutant plants for *CLE9*, *CLE16*, *CLE17*, *CLE19*, *CLE41*, *CLE42*, and *CLE45* by transforming wild-type plants separately with fusions of the *CLE* promoter and the coding region for the CLE_{G6T} point mutation (*DN-CLE*). The *DN-CLE* transgenic plants exhibited obviously reduced silique length (Fig. 2, F and G; Supplemental Fig. S5, B-G). Alexander staining and scanning electron microscopy experiments revealed abnormal anther development with aborted pollen in the anthers of these *DN-CLE* plants (Fig. 2, X, Y, AG, and AH; Supplemental Fig. S5, H–U). These results suggested that the normal functions of these genes are important for anther development and that the anther-expressed *CLE9*, *CLE16*, *CLE17*, *CLE19*, *CLE41*, and *CLE42* might function in a redundant manner. Although the DN transgenic plants of all seven *CLE* genes exhibited abnormal anther development, only the *cle19* knockout mutants showed weak anther developmental defects; therefore, we focused the subsequent detailed functional analyses on *CLE19* to gain insights into its role in anther/pollen development.

CLE19 Is Required for Normal Pollen Development, Pollen Germination, and Pollen Tube Elongation

In addition to the above-mentioned *cle19* and *DN-CLE19* mutants, we also wanted to investigate whether an increase of *CLE19* expression affects male reproductive development, using the 35S promoter-driven *CLE19* overexpression transgenic lines (*CLE19-OX*; Fiers et al., 2004). Two *CLE19-OX* transgenic lines with different *CLE19* expression levels, *CLE19-OX-S* and *CLE19-OX-M* (Fig. 3D), were selected for the analysis of anther developmental phenotypes. Both lines exhibited obviously reduced fertility, including aborted siliques, small anthers, and abnormal pollen (Fig. 2, H, I, Q, R, Z, AA, AI, and AJ).

As detected using real-time PCR, the expression level of *CLE19* was found to be elevated up to over 100-fold in the *CLE19-OX-S* line (Fig. 3D) and to a lesser extent in *DN-CLE19* anthers (Fig. 3C). The anther expression pattern of *CLE19* in the transgenic plants was examined further using RNA in situ hybridization analysis (Fig. 3, E–X). Consistently, the expression of *CLE19* was obviously increased in *CLE19-OX-S* and decreased in *cle19-2* in both tapetal and male reproductive cells (Fig. 3, J–S). However, the expression in *DN-CLE19* anthers showed no obvious difference from that in the wild type (Fig. 3, T–X), suggesting that the 35S promoter is not highly active in the tapetum and that in situ hybridization might not be quantitative enough to detect relatively small differences in expression level.

We further performed statistical analysis for various male fertility processes of the *cle19-2*, *DN-CLE19-23*, and *CLE19-OX-S* plants, including the pollen number in each anther, pollen germination and pollen tube elongation, silique length and silique number in each main stem, and seed number in each silique. Compared with the wild type, *DN-CLE19-23* produced obviously fewer pollen grains (48.4% of that in each wild-type anther), a reduced pollen germination rate (15.7% of the rate for the wild type), defective pollen tube elongation, a decreased number of siliques from one reproductive shoot, reduced silique length, and a lower

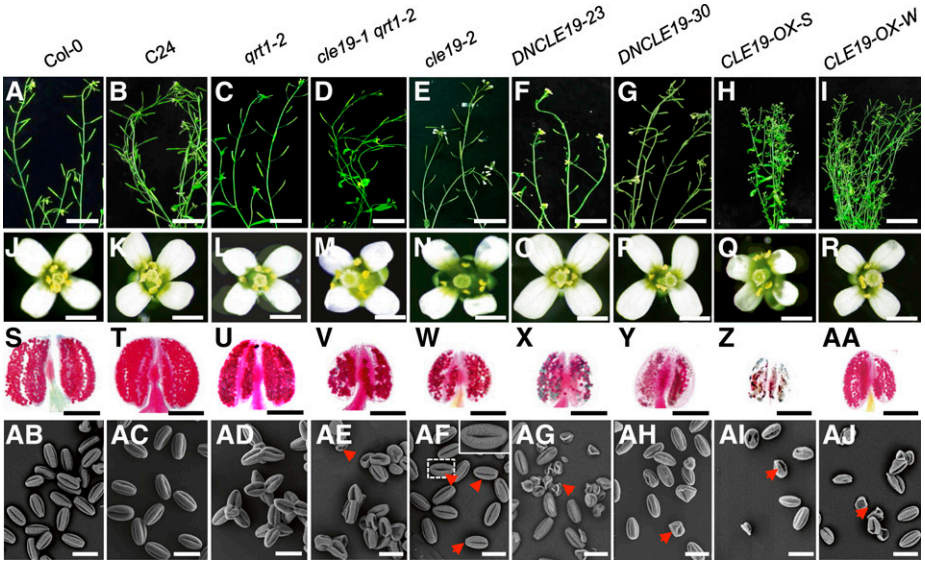

Figure 2. Phenotypic analyses of wild-type, *cle19* T-DNA insertion mutant, *DN-CLE19* transgenic, and *CLE19-OX* transgenic plants. A to I, Phenotypic analysis of plant growth of wild-type, *cle19* T-DNA insertion mutant, *DN-CLE19* transgenic, and *CLE19-OX* transgenic plants. J to R, Phenotypic analysis of flowers of wild-type, *CLE19* T-DNA insertion mutant, *DN-CLE19* transgenic, and *CLE19-OX* transgenic plants. S to AA, Phenotypic analysis of anthers of wild-type, *CLE19* T-DNA insertion mutant, *DN-CLE19* transgenic, and *CLE19-OX* transgenic plants. AB to AJ, Phenotypic analysis of pollen grains of wild-type, *CLE19* T-DNA insertion mutant, *DN-CLE19* transgenic, and *CLE19-OX* transgenic plants. Red arrowheads indicated aborted pollen grains. Bars = 2 cm for plants, 500 μm for flowers, 200 μm for anthers, and 25 μm for pollen grains.

seed number in each silique (Table I). The *cle19-1* and *cle19-2* plants exhibited similar but weaker phenotypes compared with those of *DN-CLE19*, suggesting a functional redundancy among the anther-expressed *CLE* family members, as other members also might be inhibited by the mutated CLE peptide. The *CLE19-OX-S* anther produced only 9% of the amount of pollen in one wild-type anther (Table I). All these results demonstrated the important function of *CLE19* in male reproductive processes and that the correct level of *CLE19* expression is important for normal function.

To further investigate the function of *CLE19* in anther development, particularly to identify the earliest stages when morphological differences can be observed, anther transverse semithin sections of *cle19-2*, *DN-CLE19-23*, and *CLE19-OX* mutants were examined. At anther stage 5, the wild-type anther formed well-organized five-cell layers in each anther lobe, the epidermis, endothecium, middle layer, tapetum, and microsporocytes, from outer to inner. Afterward, the microsporocytes underwent meiosis and formed the microspores that developed further into the pollen in the wild type at stages 6 to 13.

Compared with the wild type (Fig. 4, A–E), the *cle19-2* mutant anther showed no obvious cytological defects during anther stages 5 to 10, except for fewer pollen grains in the anther at stage 12 (Fig. 4, F–J). However, the *DN-CLE19-23* anthers tended to produce more than normal tapetum cells surrounding the microsporocytes at stage 5, and aborted pollen was observed at stage 10 and onward (Fig. 4, K–O). In comparison, change of the tapetal cell number was not obvious in either *CLE19-OX-S* or *CLE19-OX-M* anthers; nevertheless, most of the tapetal cells were enlarged and excessively vacuolated at stages 5 to 7, and the *CLE19-OX-S* tapetum soon degenerated at stage 8 (Fig. 4, P–R). Therefore, the development of most pollen grains was defective (Fig. 4, S and T). The *CLE19-OX-M* tapetum exhibited a weaker vacuolated morphology compared with *CLE19-OX-S* but also disappeared at stage 10. A small portion of defective pollen was observed at stage 10 and onward (Fig. 4, U–Y). These results further strengthened the idea that a proper amount of CLE19 is required for normal anther development.

Pollen Exine Formation Was Affected in *CLE19* Mutants

We then further investigated whether *CLE19* is involved in pollen exine formation. The morphological pollen exine structure of wild-type, *DN-CLE19-23*, and *CLE19-OX-S* plants was first observed using scanning electron microscopy. Pollen grains with either moderate or severe defects were analyzed in both *DN-CLE19-23* and *CLE19-OX-S* plants. The results showed that the external surface of wild-type pollen exine had a network-like structure formed with well-organized lacunae and three narrow apertures (Fig. 5, A and F). In comparison, both the moderately defective and the severely defective pollen of *DN-CLE19-23* exhibited more extensively covered surfaces with smaller lacunae filled with additional materials (Fig. 5, B, C, G, and H). In contrast, the *CLE19-OX* pollen exine exhibited clearly missing connections in the network and lack of separation between the spaces that would form the lacunae (Fig. 5, D, E, I, and J), suggesting that the proper amount of *CLE19* is required for the formation of

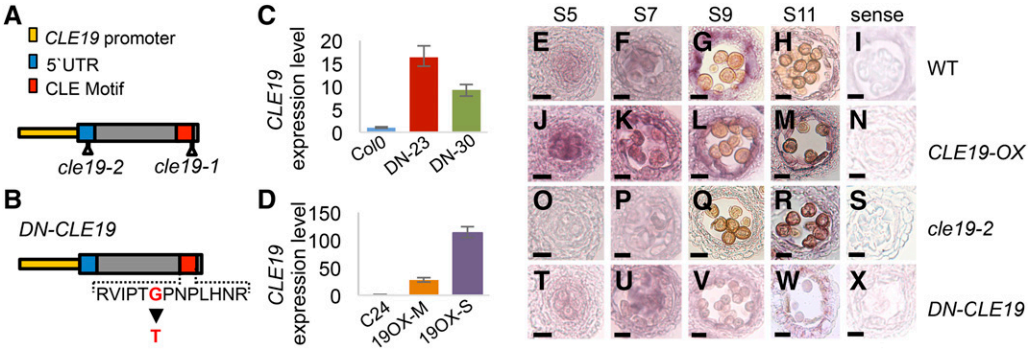

Figure 3. Spatial and temporal expression of *CLE19* in wild-type, *CLE19-OX*, *cle19-2*, and *DN-CLE19* anthers. A, Diagram showing the T-DNA insertion sites of *cle19-1* and *cle19-2*. UTR, Untranslated region. B, Diagram showing the amino acid mutation site in *DN-CLE19*. C and D, Quantitative real-time PCR analysis to detect *CLE19* expression in stage 4 to 12 anthers of the wild type, *DN-CLE19* (C), and *CLE19-OX* (D) using *EF1α* as an internal control. *DN-23* and *DN-30* indicate two individual *CLE19*::*DN-CLE19* transgenic lines. *19OX-M* and *19OX-S* indicate two independent *35S*::*CLE19* transgenic lines. Data from three biological replicates were collected. E to X, RNA in situ hybridization results showing the expression of *CLE19* in wild-type (WT), *CLE19-OX-S*, *cle19-2*, and *DN-CLE19-23* mutant anthers. Bars = 10 μm.

normal pollen exine, possibly promoting the proper organization of the network and lacunae.

Given that the pollen wall is composed of the exine and the intine layers, we further examined the characteristics of these two pollen wall layers through a diethyloxadicarbocyanine iodide- and Tinopal-based staining method. As shown in Figure 5K, the wild-type pollen exine was stained as red and the intine was stained as purple. In comparison, stronger red exine signals but minimal purple intine signals were observed in the *DN-CLE19-23* pollen grains (Fig. 5, L and M), especially in the *DN-CLE19* severe pollen grain, where little or no intine signal was observed (Fig. 5M), suggesting that *CLE19* is required for the normal formation of both pollen exine and intine. Consistently, the *CLE19-OX* pollen exhibited discrete red exine signals and irregular inward-folded purple intine fluorescence (Fig. 5, N and O). These data suggested that *CLE19* possibly negatively and positively regulates pollen exine and intine formation, respectively.

To further analyze the function of *CLE19* in pollen exine formation, transmission electron microscopy (TEM) analyses were performed. Wild-type pollen grains exhibited a uniformly structured cell wall with clearly visible exine (T-shaped bacula and tectum; Fig. 5, P and U). However, although the exine T-shaped structure of the *DN-CLE19-23* pollen appeared normal, the lacunae were filled with extra sporopollenin-like materials (Fig. 5, Q, R, V, and W). In contrast, the *CLE19-OX* exine-like layer lacked the complete bacula/tectum structure (Fig. 5, S, T, X, and Y), demonstrating that CLE19 is a negative regulator of pollen exine biogenesis, especially for the construction of the T-shaped structure.

DN-CLE19 Transgenic Plants Are Deficient in Pollen Coat Formation

As the *DN-CLE19* mutant pollen grains exhibited germination defects (Table I) and the pollen coat was filled with extra unknown substances, we assessed whether these substances result from additional synthesis or defective degradation/exploitation. Thus, the pollen coat structures of wild-type and *DN-CLE19* plants at anther stages 10 to 13 were examined. Both wild-type and *DN-CLE19* pollen in stage 10 to 11 anthers were covered with pollen coat materials, which filled the reticulate networks that surrounded the wild-type pollen; such materials were reduced and almost invisible in stage 12 to 13 wild-type pollen. Therefore, the well-organized reticulate exine networks were clearly visible on the surface of the wild-type pollen. However, these

Table I. *Phenotypic analysis of cle19-2, DN-CLE19-23, and CLE19-OX-S*

Data are means ± SD. For silique number, three replicates using 30 branches were analyzed. For silique length, three replicates and 30 siliques in each replicate were analyzed. For seed number, three replicates and 30 siliques in each replicate were analyzed. For pollen number, three replicates and more than 30 anthers in each replicate were analyzed. For pollen germination rate and pollen tube length analyses, three replicates and more than 100 pollen grains for each replicate were observed.

Plant	Silique No.	Silique Length	Seed No. per Silique	Pollen No. per Anther	Pollen Germination Rate	Pollen Tube Length
		mm			%	*μm*
Col-0	68.9 ± 3.9	14.3 ± 0.7	54.8 ± 3.6	640.3 ± 22.0	99.97 ± 5.25	208.0 ± 11.8
cle19-2	55.9 ± 3.9	13.0 ± 1.9	41.58 ± 10.1	413.6 ± 40.1	41.67 ± 5.16	137.0 ± 25.0
DN-CLE19-23	30.6 ± 3.0	10.7 ± 2.5	30.6 ± 11.5	310.2 ± 99.6	15.67 ± 4.72	82.8 ± 6.5
C24	67.2 ± 3.7	14.6 ± 1.0	48.8 ± 4.5	617.3 ± 34.9	99.96 ± 7.20	205.1 ± 9.9
CLE19-OX-S	12.9 ± 3.1	9.6 ± 2.4	22.0 ± 9.4	54.5 ± 26.7	98.53 ± 15.18	35.5 ± 8.7

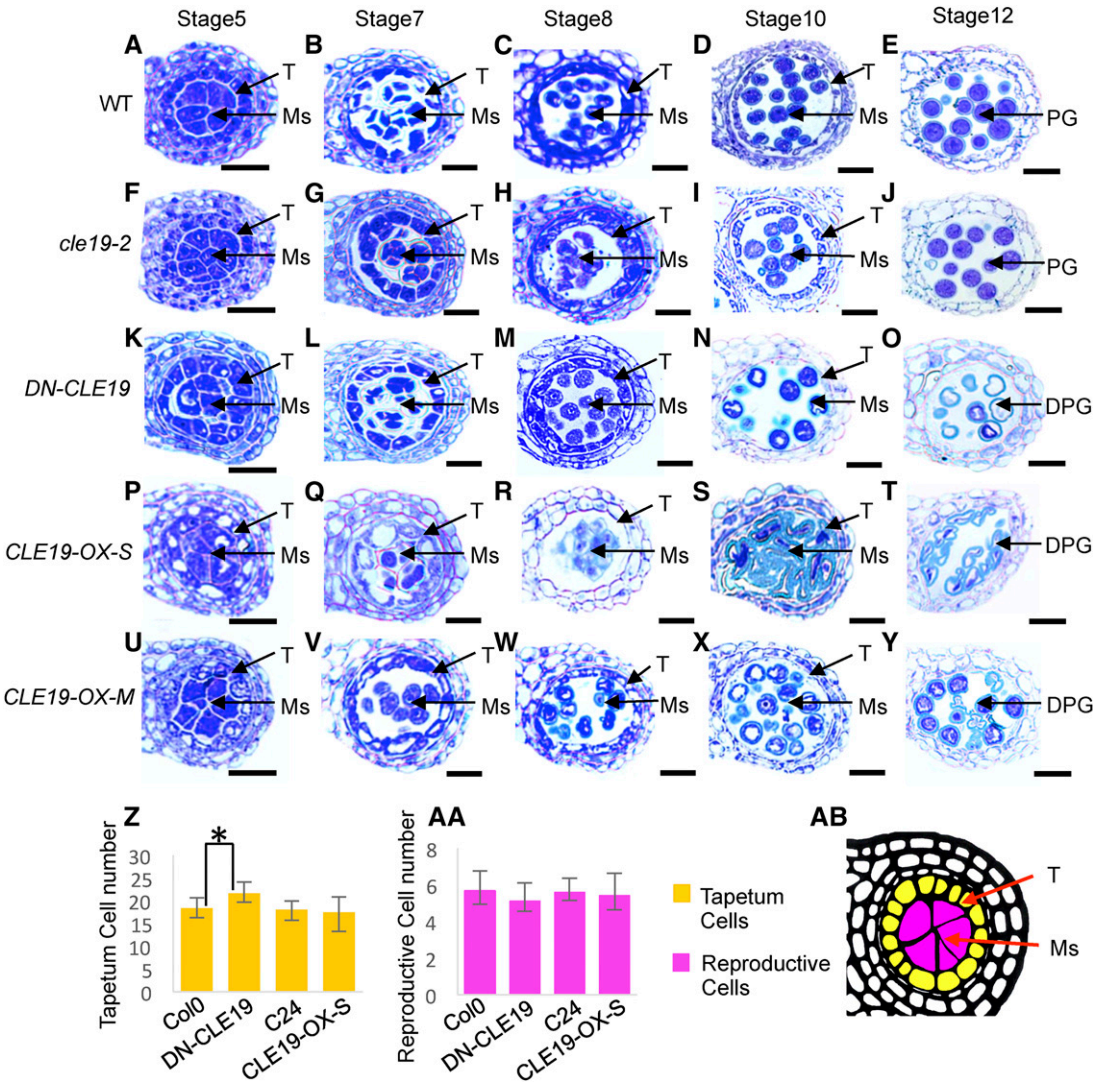

Figure 4. Cell biological analyses of wild-type, *cle19-2*, *DN-CLE19*, and *CLE19-OX* anthers. A to E, Wild-type (WT) anther morphology using semithin transverse sections. F to J, Morphology of *cle19-2* anthers using semithin transverse sections. K to O, Morphology of *DN-CLE19* anthers using semithin transverse sections. P to T, Morphology of *CLE19-OX-S* anthers using semithin transverse sections. U to Y, Morphology of *CLE19-OX-M* anthers using semithin transverse sections. Z to AA, Statistical analyses of the tapetal or reproductive cell numbers in *DN-CLE19*, *CLE19-OX*, and wild-type anthers, respectively. $*P < 0.05$ by Student's *t*-test. AB, How the numbers of tapetal or reproductive cells in each lobe in transverse sections were calculated. DPG, Degenerated pollen grains; Ms, meiocytes; PG, pollen grains; T, tapetum. Bars = 20 μm.

pollen coat materials were still present on *DN-CLE19* mutant pollen at anther stages 12 to 13 (Supplemental Fig. S6C), suggesting that the defect was in the degradation or removal of these materials.

The Expression of *AMS* and Downstream Transcription Factor Genes Was Affected in *cle19* Mutants

As the transcription factor genes *DYT1*, *MYB35/TDF*, *AMS*, *MS188/MYB103/MYB80*, and *MS1* are required for normal anther development in a *DYT1-MYB35/TDF1-AMS-MS188/MYB103/MYB80-MS1* regulatory pathway (Ge et al., 2010; Chang et al., 2011; Zhu et al., 2011) and AMS was reported to act as a master regulator coordinating pollen wall development (Xu et al., 2014), we further examined the expression levels of genes encoding these five transcription factors in *DN-CLE19* and *CLE19-OX* anthers using quantitative real-time PCR analyses. The expression levels of *AMS*, *MS188/MYB103/MYB80*, and *MS1* showed over 2-fold increases in *DN-CLE19* but over 2-fold decreases in *CLE19-OX* anthers (Fig. 6, A and B), suggesting that these genes are negatively regulated by CLE19. However, the expression of either *DYT1* or *MYB35* exhibited no obvious difference between the *DN-CLE19* and wild-type anthers, but both showed 40% reductions in

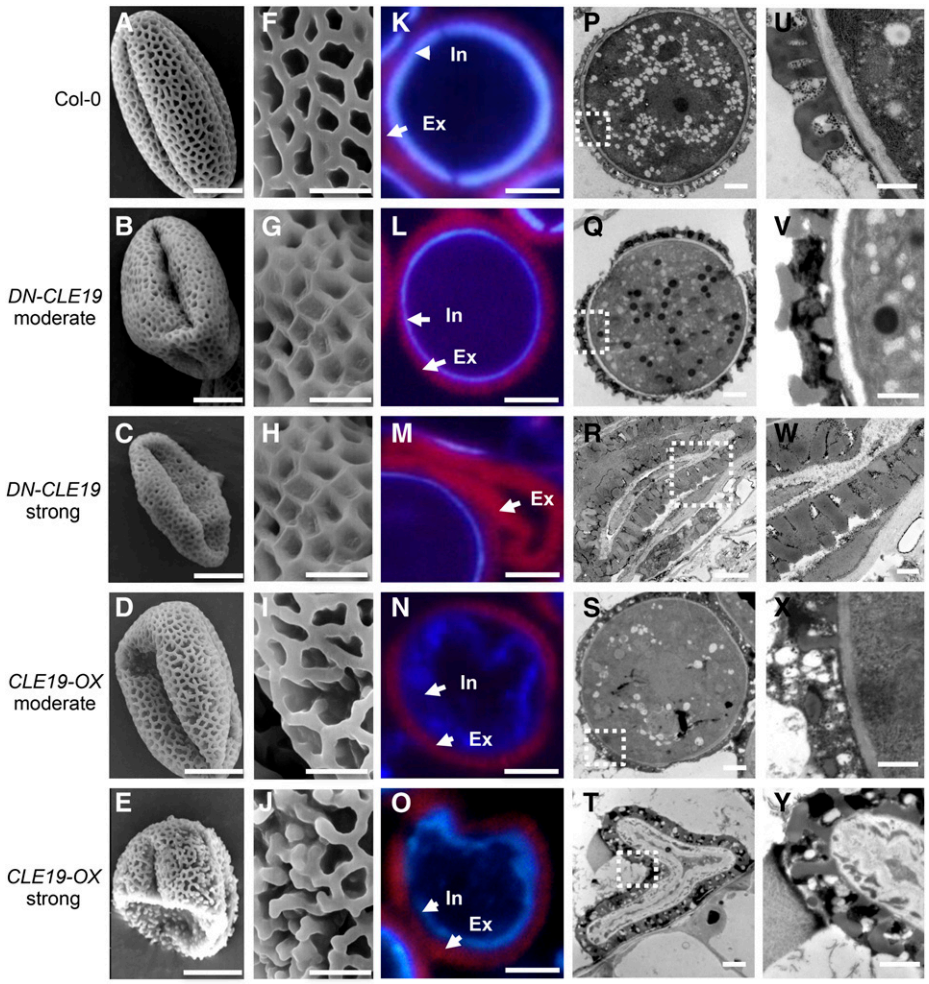

Figure 5. Microscopic analyses of wild-type, *DN-CLE19*, and *CLE19-OX* pollen exine. A to J, Pollen grains from wild-type, *DN-CLE19*, and *CLE19-OX* plants visualized by scanning electron microscopy. K to O, Cytochemical staining of semithin sections of wild-type, *DN-CLE19*, and *CLE19-OX* pollen. P to Y, Wild-type, *DN-CLE19*, and *CLE19-OX* pollen visualized by TEM. A, F, K, P, and U, Wild-type pollen. B, G, L, Q, and V, *DN-CLE19-M* pollen. C, H, M, R, and W, *DN-CLE19-S* pollen. D, I, N, S, and X, *CLE19-OX-M* pollen. E, J, O, T, and Y, *CLE19-OX-S* pollen. Ex, Exine; In, intine. Bars = 10 μm for A to E, 2 μm for F to J, 5 μm for K to O, 2 μm for P to T, and 0.5 μm for U to Y.

CLE19-OX anthers (Fig. 6, A and B), suggesting that the expression of these two genes possibly was not or was only slightly affected by *CLE19*. These results suggested that CLE19 probably functions as a negative regulator of the AMS-dependent transcriptional networks for normal pollen wall formation.

The expression of *AMS* in *DN-CLE19* and *CLE19-OX* anthers was tested further using RNA in situ hybridization analysis. The results showed that the *AMS* signal was hardly seen at anther stage 5 (Fig. 6, C and D) and was detected in both the tapetum and microsporocytes at stages 7 to 10, albeit weakly (Supplemental Fig. S7, B and C); the signal then disappeared at anther stage 12 (Supplemental Fig. S7, B and C). In comparison, *AMS* expression was obviously increased in the *DN-CLE19* transgenic anthers at anther stages 7 to 10 (Fig. 6, E and F), suggesting that inhibition of the CLE19 function caused an increase in *AMS* expression. However, no *AMS* signal was detected in *CLE19-OX* transgenic anthers at all examined stages, similar to the results in the *ams* mutant (Supplemental Fig. S7, G–P), revealing that the increased CLE19 function suppresses *AMS* expression. These data demonstrated that CLE19 acts as a negative upstream regulator of *AMS*.

CLE19-OX Anthers Had *ams*-Like Swollen Tapetal Cells

It is known that tapetal cells secrete sporopollenin precursors onto the primexine of the developing pollen for the formation of the pollen exine and that AMS plays an important role in this process, with *ams* showing severely swollen tapetal cells with large vacuoles and few lipidic tapetosomes and elaioplasts (Xu et al., 2014). We postulated that, if CLE19 acts as a negative upstream regulator of AMS, tapetal cells of the *CLE19-OX* anther would exhibit similar abnormal phenotypes to that of *ams*. Therefore, we performed TEM analysis of *CLE19-OX* tapetal cells. As expected, in contrast to the condensed and degenerated cytoplasm of wild-type tapetal cells, with evident disintegration of cell membrane and accumulation of lipidic tapetosomes and elaioplasts (Fig. 6G), *CLE19-OX* tapetal cells were highly vacuolated and swollen, with large vacuoles and lack of lipidic tapetosomes and elaioplasts (Fig. 6H). In addition, sporopollenin precursors on the primexine were clearly observed on the outer surface of wild-type pollen grains; however, no obvious accumulation of sporopollenin precursors was seen on the primexine of the *CLE19-OX* (Fig. 6, I and J) and *ams* (Fig. 6, K and L) pollen grains.

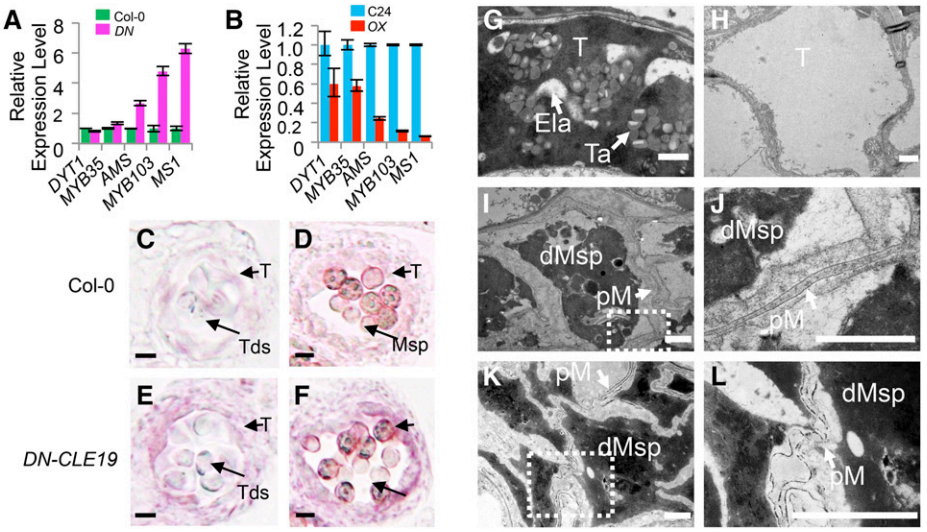

Figure 6. Quantitative real-time PCR and RNA in situ hybridization analyses to test the expression of *AMS* and downstream transcription factor genes in *DN-CLE19* and *CLE19-OX* transgenic anthers, and TEM observation of *CLE19-OX* and *ams* tapetal cells and microspores. A and B, Relative expression levels of the transcription factor genes *DYT1*, *MYB35*, *AMS*, *MYB103*, and *MS1* in *DN-CLE19* and *CLE19-OX* mutants compared with related wild-type plants, with *ACTIN* expression as an internal control. C and D, Expression of *AMS* in wild-type anthers. E and F, Expression of *AMS* in *DN-CLE19* anthers. C and E show anther stage 7, and D and F show anther stage 10. G to L, Tapetal cells of wild-type and *CLE19-OX-S* anthers visualized by TEM. G, The wild type. H, *CLE19-OX-S*. I to L, Microspore cells of *CLE19-OX-S* and *ams* anthers visualized by TEM. I and J, *CLE19-OX-S*. K and L, *ams*. dMsp, Degenerated microspores; Ela, elaioplasts; pM, primexine; T, tapetum; Ta, tapetosomes. Bars = 1 μm.

Altered Expression of 1,711 and 2,188 Genes in *DN-CLE19* and *CLE19-OX* Anthers, Respectively

To further investigate the *CLE19* effects on anther transcriptomes, those of stage 4 to 10 anthers were assessed (Supplemental Fig. S8, A and B). Compared with the wild type, 578 (34% of the total of 1,711 differentially expressed genes) were down-regulated and 1,133 (66%) were up-regulated in the *DN-CLE19* anthers (Fig. 7, A and B; Supplemental Data Set S1). Moreover, the expression of 1,809 genes was down-regulated and that of 379 genes was up-regulated (83% and 17% of the 2,188 total altered genes, respectively) in the *CLE19-OX* anthers (Fig. 7, A and B; Supplemental Data Set S2). The fact that most of the differentially expressed genes were up-regulated in the loss-of-function *DN-CLE19* mutant and down-regulated in the gain-of-function *CLE19-OX* mutant suggests that *CLE19* negatively regulates anther gene expression. Interestingly, the expression of 742 genes was both up-regulated in *DN-CLE19* and down-regulated in *CLE19-OX* (Fig. 7C; Supplemental Data Set S3), while only 52 genes were both down-regulated in *DN-CLE19* and up-regulated in *CLE19-OX* transcriptomes (Fig. 7D; Supplemental Data Set S4), further supporting CLE19 functioning as a negative regulator of many anther genes.

The Expression of 280 AMS-Downstream Genes Was Affected in Both *DN-CLE19* and *CLE19-OX* Mutants

Considering the similar developmental defects of tapetum of *CLE19-OX* and the *ams* mutant, we further compared the 923 genes that were commonly regulated in *DN-CLE19* and *CLE19-OX* in our transcription data sets with the microarray-based *ams* transcriptomic data of the stage 4 to 7 anther and buds of four anther developmental stages (Xu et al., 2010; Feng et al., 2012; Ma et al., 2012). The results revealed that the expression of 135 out of the 923 *CLE19* downstream genes also was altered in the *ams* stage 4 to 7 anthers and that of 201 also was altered in various stages of *ams* buds (Fig. 6E; Supplemental Data Set S5). The combined set included a total of 280 genes commonly affected by both *CLE19* and *AMS*; the putative functions of these genes are enriched in various biological processes, including pollen exine formation, sexual reproduction, lipid transport, lipid storage, and lipid metabolism (Fig. 7F), suggesting that *CLE19* likely functions through *AMS-MYB103/MYB80-MS1* pathways, but probably not through the more upstream regulators *DYT1* and/or *MYB35*, to regulate the transcriptional networks important for pollen exine formation (Fig. 7G).

CLE19 Controls the Synthesis of Lipidic and Phenolic Components and Flavonoids Required for Pollen Wall Formation

Sporopollenins are the major components of pollen exine. Increasing evidence indicates that sporopollenin consists mainly of complex aliphatic monomers, including very-long chain fatty acids and their polyhydroxylated derivatives, as well as phenolic compounds (Kim and Douglas, 2013). Lipid metabolism and transport genes are highly expressed in the pollen compared with vegetative

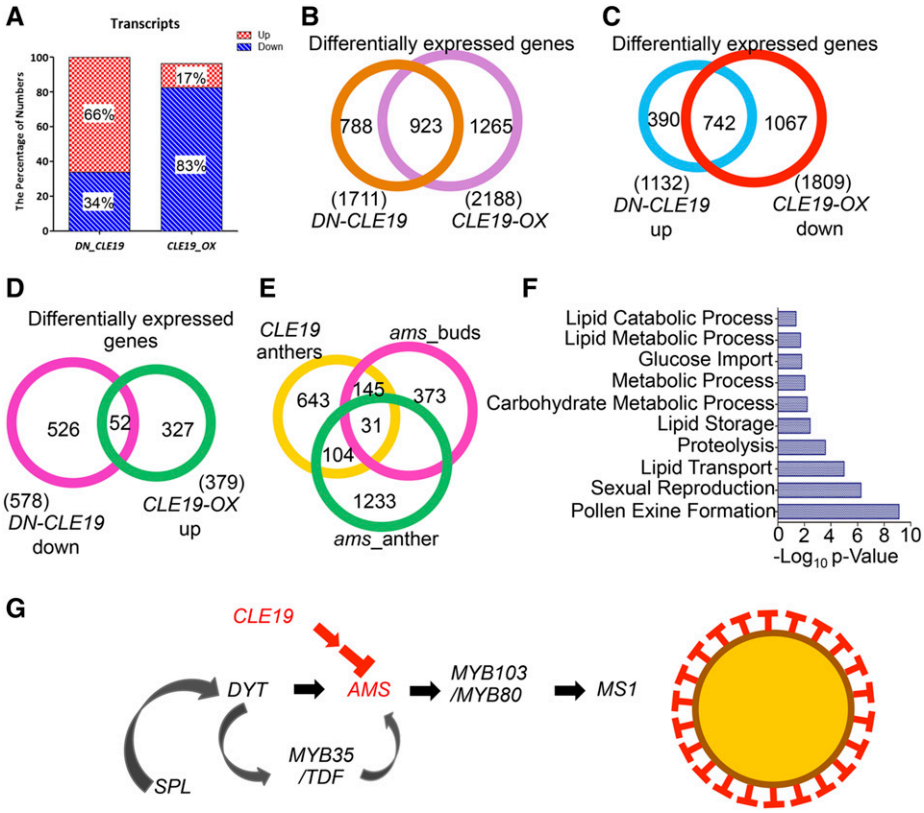

Figure 7. Transcriptomic comparison analyses between *CLE19* and *AMS*. A, Percentages of up- and down-regulated genes in the *DN-CLE19* and *CLE19-OX* transcriptomes, respectively. B, Comparison of differentially expressed genes between *DN-CLE19* and *CLE19-OX* transcriptomes. C, Comparison of differentially expressed genes between *DN-CLE19* up-regulated and *CLE19-OX* down-regulated gene groups. D, Comparison of differentially expressed genes between *DN-CLE19* down-regulated and *CLE19-OX* up-regulated gene groups. E, Venn diagram showing the overlap between genes affected in *CLE19* anthers, *ams* floral buds, and *ams* anthers. F, Enriched biological process categories for transcriptome analysis of genes affected in both *CLE19* and *ams* mutants. G, *CLE19* genetic pathways controlling anther development.

tissues, suggesting important roles of lipid metabolism in pollen development (Honys and Twell, 2004). Among the differentially expressed genes, many are involved in the pollen coat and exine formation, as determined by previous studies (Wilson and Zhang, 2009; Ariizumi and Toriyama, 2011), contributing to the synthesis of pollen coat precursors and sporopollenin. It is generally understood that sterol esters and saturated acyl groups are the major components of the pollen coat, similar to those of lipid or oil droplets but different from lipids of biological membranes.

As developmental defects were observed in both tapetal cells and pollen wall in *CLE19* mutants, we analyzed the expression of genes implicated in lipid acyl metabolism, including the metabolism of flavonoids, phenolics, free fatty acids, wax ester, and cutin (Fig. 8A), and found that 36 lipid acyl metabolism-related genes showed more that 2-fold differences in expression between *DN-CLE19* and/or *CLE19-OX* mutant anthers. Among these, 20 genes also were altered in expression in *ams* anthers and/or floral buds (Ma et al., 2012; Xu et al., 2014). Importantly, 19 out of the 20 coregulated genes showed changes in expression in the opposite direction: up-regulated in the *CLE19-DN* mutant but down-regulated in *CLE19-OX* and *ams* mutants (Fig. 8, B–F). These results suggest that *CLE19* mediates the tapetum and pollen wall developmental signaling pathways by negatively regulating the expression of these genes, with at least some dependence on *AMS* function.

The *ams* Mutation Partially Suppressed *DN-CLE19*-Induced Abnormal Anther Development and Pollen Exine Formation

To test the hypothesis that CLE19 functions with at least some dependence on AMS function, we generated *DN-CLE19(+/+) ams(+/−)* and *DN-CLE19(+/+) ams(−/−)* plants by crossing the *DN-CLE19-23* homozygous plant [*DN-CLE19-23(+/+)*] with the *ams* mutant and observed the pollen exine structure of each genotype. Compared with the wild-type anthers containing pollen with a well-organized pollen exine structure (Fig. 9, A and F), *ams* produced smaller anthers without any pollen (Fig. 9B) and *DN-CLE19-23* produced slightly smaller anthers and fewer pollen grains, with some pollen grains being aborted (Fig. 9, C and G–I). Interestingly, the *DN-CLE19(+/+) ams(+/−)* anthers were even smaller than the *DN-CLE19* anthers, with few pollen grains (Fig. 9D); the *DN-CLE19(+/+) ams(−/−)* anthers were similar to the *ams* anthers (Fig. 9E).

To further investigate the genetic interaction between *CLE19* and *AMS*, we then compared the pollen exine structure between pollen grains from the *DN-CLE19* and *DN-CLE19(+/+) ams(+/−)* plants. As both the *DN-CLE19* and *DN-CLE19(+/+) ams(+/−)* plants produced pollen grains with pollen exine defects with different degrees of severity, we classified the defects into three levels: slight (Fig. 9, G and J), moderate (Fig. 9, H and K), and severe (Fig. 9, I and L) defects. Statistical analysis showed that, after the *ams(+/−)* genotype was

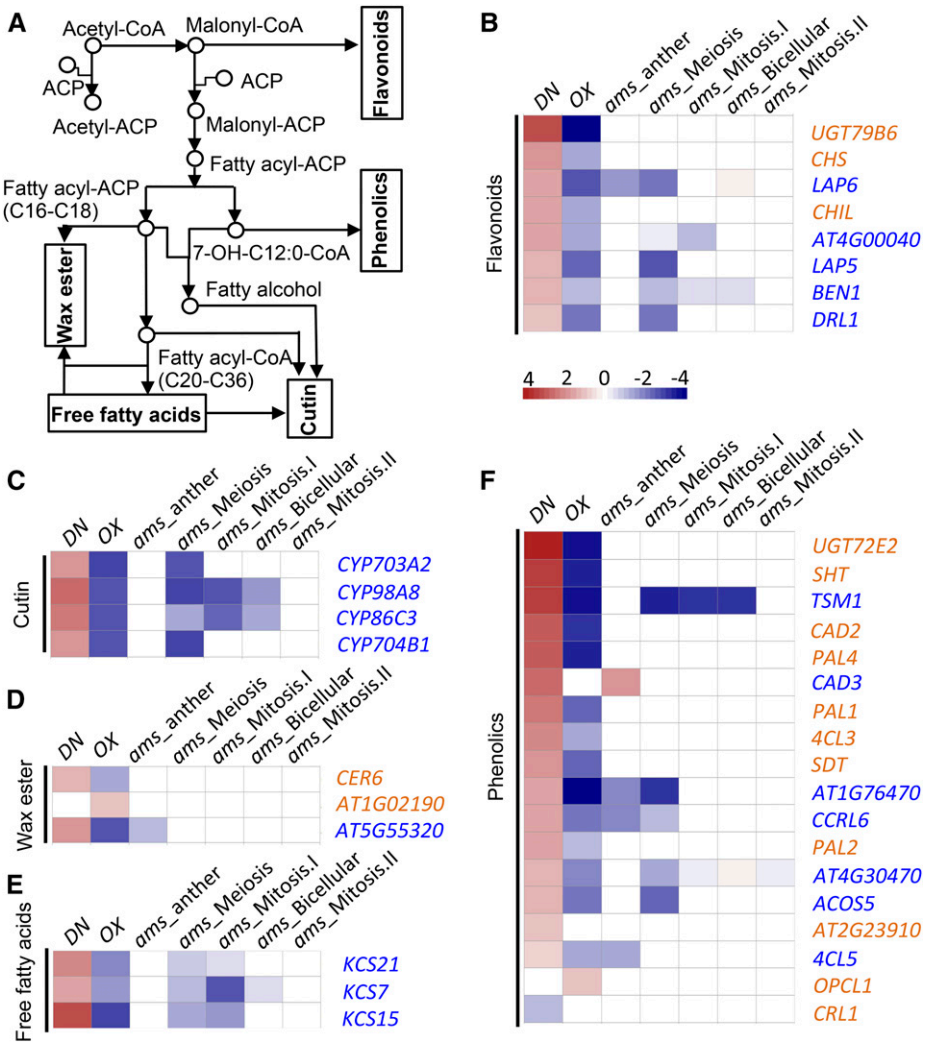

Figure 8. Transcriptomic analyses of genes involved in the metabolism of flavonoids, phenolics, wax, cutin, and free fatty acids in the wild type and the *CLE19* mutant. A, Metabolic processes of the main compounds of the pollen wall. B to F, Fold changes in expression levels of genes involved in flavonoid metabolic, cutin metabolic, wax ester metabolic, free fatty acid metabolic, and phenolic metabolic processes.

introduced into the *DN-CLE19* plants, the percentage of severely defective pollen was obviously reduced (from 32.9% to 22.4%; Fig. 9M) and the percentages of pollen with moderate defects and slight defects were increased (from 26.5% to 35.5% and from 40.6% to 42.1%, respectively; Fig. 9M), demonstrating that CLE19 works in a way dependent on the AMS function.

DISCUSSION

A Proper Amount of CLE19 Is Important for Pollen Wall Formation

Cell-cell communication is often mediated by the extracellular ligands and their receptors and is essential for the development of multicellular organisms, including anther development in angiosperms (Zhao et al., 2002; Yang et al., 2003, 2016; Jia et al., 2008; Huang et al., 2016). During pollen development, the adjacent tapetal layer provides metabolites and sporopollenin precursors for pollen coat and exine formation as well as signals essential for pollen development (Mariani et al., 1990; Goldberg et al., 1993; Sanders et al., 1999). The pollen mother cells surrounded by the tapetum undergo meiosis and form a tetrad enveloped by a thick protective callose (1,3-β-glucan) wall that is digested subsequently by glucanases secreted from the tapetum, resulting in the release of microspores. Then, the microspores develop into mature pollen grains with the deposition of lipidic precursors/components secreted by the tapetal cells onto the pollen surface to form the pollen exine and pollen coats (Mascarenhas, 1975; Stieglitz, 1977; Pacini and Juniper, 1979). The signaling communication between tapetal cells and the reproductive cells (including pollen mother cells and developing pollen grains) is important for normal anther development and pollen formation. For instance, Arabidopsis reproductive cell-preferential TPD1 and the tapetum-expressed EMS1 and SOMATIC EMBRYOGENESIS RECEPTOR-LIKE KINASE1/2 (SERK1/2) complex interact to regulate normal tapetum differentiation and pollen development, and plants with mutations in *TPD1*, *EMS1*, or *SERK1/2* produce no microspores (Zhao et al., 2002; Yang et al., 2003; Albrecht et al., 2005; Huang et al., 2016; Li et al., 2017).

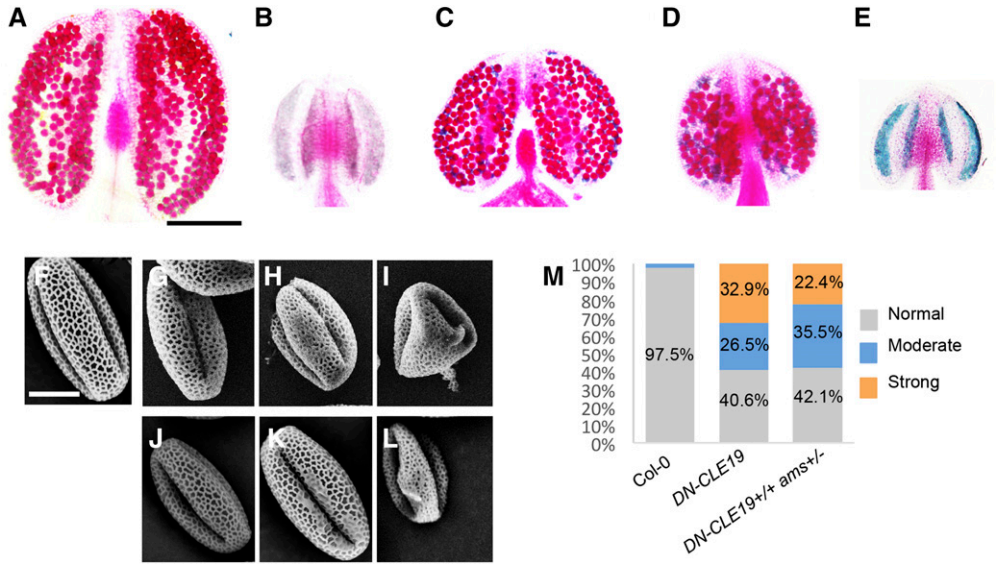

Figure 9. Phenotypic analysis of anthers from wild-type, *ams* mutant, *DN-CLE19* transgenic, *DN-CLE19(+/+) ams(+/−)*, and *DN-CLE19(+/+) ams(−/−)* plants. A to E, Alexander-stained anthers from wild-type (A), *ams* mutant (B), *DN-CLE19* transgenic (C), *DN-CLE19(+/+) ams(+/−)* (D), and *DN-CLE19(+/+) ams(−/−)* (E) plants. F to L, Pollen grains from wild-type (F), *DN-CLE19* transgenic (G–I), and *DN-CLE19(+/+) ams(+/−)* (J–L) plants. M, Statistical analysis data to show the percentage of pollen grains with abnormal exine in wild-type, *DN-CLE19* transgenic, and *DN-CLE19(+/+) ams(+/−)* plants. Bars = 200 μm for anthers and 10 μm for pollen grains.

However, the functions of extracellular ligand and RLK-mediated signaling pathways in the regulation of pollen development are rarely reported.

In this study, using combined strategies of cell biology, genetics, and transcriptomics, we found that *CLE19* is required for the normal development of pollen, especially for the normal biogenesis of pollen exine. All *CLE19* mutant lines exhibited abnormal pollen development with a portion of pollen grains aborted; however, pollen exine structures exhibited differences among mutants with different *CLE19* expression levels. Unlike the wild-type pollen grains that are covered by a well-organized network-like lacunae structure, the *cle19-2* and *DN-CLE19* pollen grains had a more extensively covered surface with broader muri and smaller lacunae units, and most of the lacunae units were filled with extra sporopollenin-like substances (Fig. 5). In contrast, the *CLE19-OX* pollen grains exhibited a shortage of the characteristic reticulate structures composed of bacula and tectum (Fig. 5), suggesting that the lacunae of pollen exine were incomplete. Further transcriptomic analyses revealed that the expression of numerous genes involved in pollen wall assembly, lipid metabolism, transport, and localization were up-regulated in *DN-CLE19* but down-regulated in *CLE19-OX* anthers (Figs. 7 and 8), demonstrating that *CLE19* functions as a negative regulator of these genes. These data suggested that a proper amount of the CLE19 signal is essential for the normal organization of the pollen wall, and either more or less than the normal level of *CLE19* would destroy the balance of both the expression of pollen developmental genes and the construction of normal pollen exine.

CLE19 Functions as a Negative Regulator of AMS-Regulated Pollen Wall Developmental Pathways

Previous studies have demonstrated that the transcription factors DYT1, MYB35/TDF1, AMS, MYB103/MYB80, and MS1 are required for anther development and that they form a genetically defined pathway/regulatory cascade: *DYT1-MYB35/TDF1-AMS-MYB103/MYB80-MS1* (Zhu et al., 2011). AMS is a key regulator of sporopollenin biosynthesis, secretion, and pollen wall formation and can form a complex with MS188/MYB103/MYB80 that likely activates the expression of *CYP703A2* and *MS1* encoding a transcription factor (Xu et al., 2010, 2014; Zhu et al., 2011; Feng et al., 2012; Gu et al., 2014; Xiong et al., 2016; Ferguson et al., 2017). DYT1 and MYB35/TDF1 are required for the development of tapetum and reproductive cells at early stages, as supported by the findings that *DYT1* and *MYB35/TDF1* mutants exhibit abnormal tapetal cells at anther stage 5 and onward and that their anthers lack any pollen (Zhang et al., 2006; Zhu et al., 2008; Gu et al., 2014). These two genes are important for normal anther and pollen development, at least in part by activating the normal expression of *AMS*. In our study, we showed that *CLE19* negatively regulates the expression of *AMS* and the downstream genes *MYB103/MYB80* and *MS1* to prevent their deleterious overexpression, but it does not obviously affect the normal expression of DYT1 and MYB35/TDF1 (Fig. 6), demonstrating that *CLE19* probably functions to modulate the proper level of the activity of the AMS-regulated network and the appropriate amount of sporopollenin biosynthesis and pollen wall formation. The cytological results that both *CLE19-OX* transgenic anthers and the *ams* mutant anthers

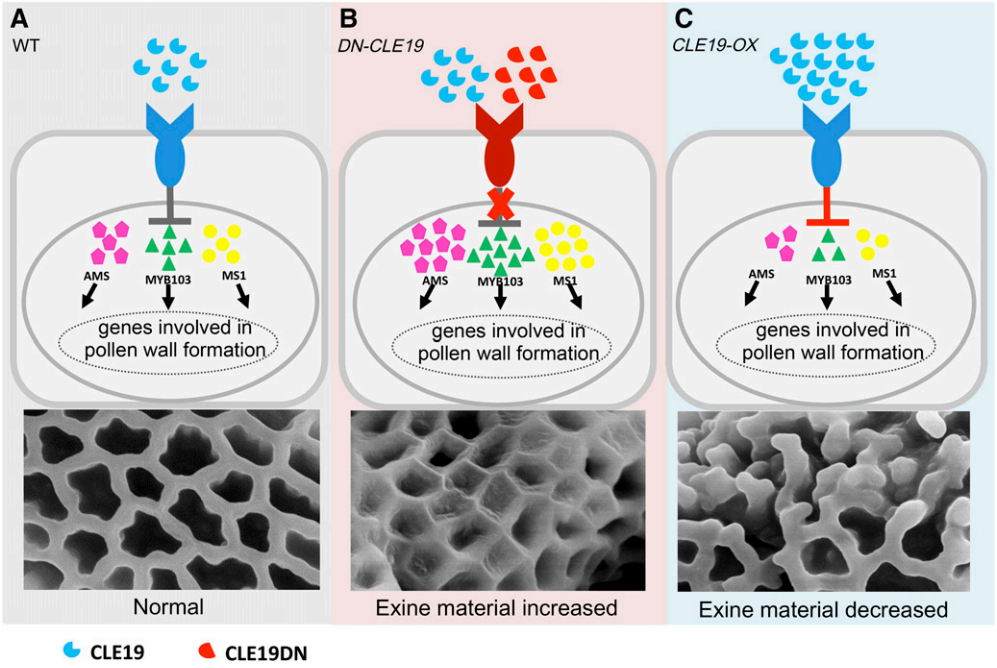

Figure 10. Proposed working model for CLE19 in the regulation of anther development. A, In wild-type anthers, CLE19 peptides interact with their unknown receptor to negatively regulate the AMS-MYB103-MS1 transcriptional cascade to prevent their deleterious overexpression, which triggers the normal expression of downstream exine formation-related genes, and subsequently regulate the formation of normally well-organized pollen exine. B, In *DN-CLE19* anthers, CLE19 peptides without function competitively interact with the unknown CLE19 receptor, which blocks or obviously reduces signal transduction from the functional CLE19 to its downstream molecules, leading to the deleterious overexpression of the AMS-MYB103-MS1 transcriptional cascade and downstream exine formation-related genes, and subsequently affect normal pollen exine formation. C, In *CLE19-OX* anthers, overexpression of CLE19 peptide strengthens the suppression of transcription factor gene expression, resulting in abnormal pollen exine formation.

showed similar abnormal tapetum cells and pollen primexine developmental defects, and the genetic result that *ams(+/−)* partially suppressed the *DN-CLE19* transgene-induced pollen exine defects (Fig. 9), together support the ideas that AMS works downstream of the CLE19 signaling pathway and that the full effect of CLE19 depends on the normal level of AMS.

Therefore, we propose that the CLE19 peptide, probably through unknown plasma membrane-localized receptor(s), negatively regulates the AMS-MYB103-MS1 transcriptional cascades to maintain their functional homeostasis and ensure the normal development of pollen (Fig. 10A). However, in the *DN-CLE19* mutants, the reduced function of CLE19 releases the transcriptional inhibition and causes the deleterious overexpression of *AMS* and downstream networks; such overexpression then subsequently affects the normal organization of pollen exine (Fig. 10B). In contrast, in the *CLE19-OX* anthers, CLE19 synthesized at abnormally high levels excessively inhibits the expression and function of *AMS* and downstream networks, thereby inducing abnormal pollen development (Fig. 10C).

Functional Redundancy between Anther-Expressed *CLE* Genes

As an extracellular peptide hormone, CLE19 was expressed at relatively low levels in the inflorescence and stage 4 to 12 anthers in our quantitative real-time PCR analysis using *EF1α* as the internal control (Supplemental Fig. S1B). Nevertheless, both *CLE19-OX* and *DN-CLE19* transgenic plants showed obviously male fertility defects, even though the *cle19* single mutants showed weak anther developmental defects (Fig. 2). We would like to offer the following thoughts. First, RNA in situ hybridization analysis results showed that *CLE19* was expressed only in the tapetal and male reproductive cells at anther stages 5 to 7 (Fig. 1, M–P), suggesting strong cell specificity and a short duration of *CLE19* expression in the anther. We believe that both the high cell specificity and the short duration of *CLE19* expression contribute to its signal being diluted by nonexpressing cells in the inflorescence or stage 4 to 12 anthers. Second, as supported by the results here, CLE19 acts as a negative regulator of *AMS* and additional downstream genes, which are required for normal tapetum function and pollen development. If *CLE19* is allowed to be expressed at very high levels, normal pollen development would be inhibited, as seen in the *CLE19-OX* plants.

It is challenging to obtain mutants of *CLE* genes because they are all small genes; in addition, the anther-expressed *CLE* genes might have overlapping (redundant) functions. In this study, knockout mutants of five anther-expressed *CLE* genes, *CLE9*, *CLE16*, *CLE17*, *CLE19*, and *CLE42*, were characterized briefly, and only *CLE19* knockout mutants exhibited very weak anther developmental defects, whereas

mutants of the other four genes showed no obvious developmental or fertility defects. Nevertheless, our statistical analysis results showed that, compared with the wild-type plants, their double and triple mutants showed several detectable defects: increased barren silique number, reduced total pollen number but increased aborted pollen number in each anther, and increased percentage of pollen with abnormal pollen exine structure (Supplemental Fig. S4; Supplemental Table S1). In addition, the DN transgenic mutants of these seven anther-expressed *CLE* members, *DN-CLE9*, *DN-CLE16*, *DN-CLE17*, *DN-CLE19*, *DN-CLE41*, *DN-CLE42*, and *DN-CLE45*, all showed severe anther developmental and pollen exine formation defects (Supplemental Fig. S5). All these results suggested that these anther-expressed *CLE* members possibly function in a redundant way in the regulation of male fertility, especially in the regulation of pollen exine formation. We believe that further studies with various multiple mutants may uncover the details of redundant and distinctive functions on different developmental aspects between these *CLE* members.

In addition, further studies also are needed to uncover additional signaling components in the complex network that regulates pollen wall formation. For example, what is the RLK that perceives the CLE peptide signal and transduces the signal into the cytoplasm? What are the downstream effectors, such as kinase and other factors, that respond to the CLE-RLK signaling module, and how do they activate the AMS transcription factor? What is the proper amount of CLE peptide? Further investigations using a combination of omics, biochemistry, cell biology, and genetic strategies may answer these questions and further advance the study of male fertility.

CONCLUSION

In summary, our observations demonstrated that *CLE19* is essential for normal anther development and pollen wall formation, likely and in large part by negatively regulating the expression of *AMS* and the downstream genes *MYB103/MYB80* and *MS1* to prevent their deleterious overexpression, and to modulate the proper level of the activity of the AMS-regulated network and the appropriate anther development and pollen wall formation.

MATERIALS AND METHODS

Plant Growth and Genotyping

Arabidopsis (*Arabidopsis thaliana*) plants were grown on soil in greenhouse conditions (21°C) under long-day conditions (16 h of light/8 h of dark). T-DNA insertion mutant alleles of *cle19* (CS879453 and CS321816), *cle9* (SALK_018122C), *cle17* (SALK_103714C), and *cle42* (SALK_057407C) mutants and RNAi plants of *CLE16* (CS201209) in the Col-0 background were all obtained from Arabidopsis Biological Resource Center stocks. The T-DNA insertion of *CLE19* alleles was verified using the T-DNA border primer SALKLB1.3 in combination with the gene-specific primers listed in Supplemental Table S2.

Molecular Cloning and Generation of Transgenic Plants and Genotyping

Genomic sequences of *CLE9*, *CLE16*, *CLE17*, *CLE19*, *CLE41*, *CLE42*, and *CLE45* were cloned into the pDONR221 vector (Life Technologies) with the primers list in Supplemental Table S3. Using a PCR-based site-directed mutagenesis kit (Transgene) and specific primers (Supplemental Table S3), the Gly codon at the sixth position of the CLE motif of these CLE genes was replaced by the Thr codon, producing pDONR221-CLE9$_{G6T}$, pDONR221-CLE16$_{G6T}$, pDONR221-CLE17$_{G6T}$, pDONR221-CLE19$_{G6T}$, pDONR221-CLE41$_{G6T}$, pDONR221-CLE42$_{G6T}$, and pDONR221-CLE45$_{G6T}$ entry clones. These entry clones were then subcloned into the pBGWFS7 binary vector (Karimi et al., 2002) to produce CLE19$_{G6T}$, *CLE19*$_{G6T}$, *CLE16*$_{G6T}$, *CLE17*$_{G6T}$, *CLE41*$_{G6T}$, *CLE42*$_{G6T}$, and *CLE45*$_{G6T}$. Transformation was performed via an *Agrobacterium tumefaciens*-mediated floral dip method (Clough and Bent, 1998). Transgenic plants were obtained under the selection of 25 mg of Basta (Sigma-Aldrich).

Quantitative Real-Time PCR Analysis

To analyze the expression levels of the *CLE*s and other downstream genes, stage 1 to 11 flower buds of Col-0, each related T-DNA or RNAi mutant, and DN-CLE transgenic plants were collected, and total RNA was extracted according to a Trizol-based (Sigma-Aldrich) method. After DNase I digestion and first-strand cDNA synthesis, quantitative real-time PCR was performed with SYBR premix Ex Taq II (Takara) on the ABI StepOnePlus real-time system (Life Technologies) using the primers listed in Supplemental Table S4 and with *EF1a* (AT5G60390) as the internal control.

RNA in Situ Hybridization

RNA in situ hybridization analysis was performed using the Digoxigenin RNA Labeling Kit (Roche) and the PCR DIG Probe Synthesis Kit (Roche). cDNA fragments of target genes about 400 bp were amplified using the specific primers listed in Supplemental Table S5. PCR products were cloned into the pGEM-T vector and confirmed by sequencing. Completely digested plasmid DNAs were used as the template for transcription with T7 or SP6 RNA polymerase.

Phenotypic Analysis of Flowers and Anthers

Plants were photographed with a digital camera (Canon). Flower images were taken with the SPOT FLEX digital camera (Diagnostic Instruments) using the SteREO Discovery V8 dissecting microscope (Carl Zeiss Microimaging).

Stage 12 anthers were collected and stained overnight at room temperature using the Alexander solution prepared following a published protocol (Alexander, 1969), and additional anthers were pressed to release the stained pollen grains and photographed by an AXIO ScopeA1 microscope (Carl Zeiss Microimaging) with a Axio Cam HRc camera (Carl Zeiss Microimaging).

Light and Electron Microscopy Observation

Inflorescences of wild-type and mutant plants were collected and fixed in FAA (formaldehyde–acetic acid–ethanol) solution and embedded in Technovit 7100 resin (Heraeus Kulzer) as described (Jin et al., 2013). Semithin sections were prepared by cutting inflorescence materials into 1-μm-thick sections using a motorized RM2265 rotary microtome (Leica Microsystems) and then were stained with 0.05% Toluidine Blue O for 15 to 30 min and photographed by bright-field microscopy.

For pollen wall observation, sections were stained with Toluidine Blue for 5 min (10 mg mL^{-1}), Tinopal for 15 min (10 μg μL^{-1}; Sigma-Aldrich), and diethyloxadicarbocyanine iodide for 5 min (5 μL mL^{-1}; Sigma-Aldrich), and sample photographs were taken using an AXIO ScopeA1 microscope with a 390- to 440-nm excitation filter and a 478-nm blocking filter.

For scanning electron microscopy examination, fresh pollen grains released from stage 13 anthers were coated with gold and observed with an SU8010 microscope (Hitachi).

For TEM observation, different stage buds were fixed in glutaric dialdehyde buffer and embedded into the fresh mixed resin. Ultrathin sections (70-100 nm thick) were observed with a Tecnai G2 Spirit TWIN transmission electron microscope (FEI).

RNA-seq and Data Analysis

More than 1,000 stage 4 to 10 anthers from wild-type and mutant plants were collected and immediately frozen in liquid nitrogen. Total RNA from each sample was extracted and purified using the ZR Plant RNA Miniprep Kit (Zymo Research). Two micrograms of total RNA of each sample was used for deep sequencing by an Illumina HiSeq 2000 system. All sequencing data were mapped and analyzed following the previously reported method (Zhu et al., 2015).

Accession Numbers

The original RNA-seq data from this article have been submitted to the National Center for Biotechnology Information Gene Expression Omnibus database under accession number GSE94607. Sequence data from this article can be found in the Arabidopsis Genome Initiative database under the following accession numbers: *CLE9* (At1g26600), *CLE16* (At2g01505), *CLE17* (At1g70895), *CLE19* (At3g24225), *CLE42* (At2g34925), *CLE45* (At1g69588), *DYT1* (At4g21330), *AMS* (At2g16910), *MYB35/TDF1* (At3g28470), *MS1* (At5g22260), *MYB103* (At1g63910), *EF1α* (At5g60390), and *ACT2* (At3g18780). Germplasm used included *cle9-1* (SALK_018122C), *cle16-1* (CS201209), *cle17-1* (SALK_103714C), *cle19-1* (CS879453), *qrt1-2* (SALK_CS8846), *cle19-2* (CS321816), and *cle42-1* (SALK_057407C).

Supplemental Data

The following supplemental materials are available.

Supplemental Figure S1. Expression patterns of *CLE* genes in various Arabidopsis organs.

Supplemental Figure S2. T-DNA locations or RNAi targeting sites and relative expression of detected genes in the *cle9-1*, *cle16-1*, *cle17-1*, *qrt1-2*, *cle19-1 qrt1-2*, *cle19-2*, and *cle42-1* mutants.

Supplemental Figure S3. Phenotypic analyses of plant growth, anthers, and pollen of wild-type and *cle9-1*, *cle16-1*, *cle17-1*, *qrt1-2*, *cle19-1 qrt1-2*, *cle19-2*, and *cle42-1* plants.

Supplemental Figure S4. Phenotypic analyses of siliques, flowers, anthers, and pollen grains in the wild type and the *cle* single, double, and triple mutants.

Supplemental Figure S5. Phenotypic analyses of plant growth, anthers, and pollen grains of wild-type and DN-CLE transgenic plants.

Supplemental Figure S6. Comparison of exine patterns among *cle19-2*, *DN-CLE19*, *DN-CLE41*, *DN-CLE42*, and the wild type.

Supplemental Figure S7. RNA in situ hybridization analysis to detect the spatial and temporal expression of the *AMS* gene in wild-type, *ams*, *DN-CLE19*, and *CLE19-OX* transgenic anthers.

Supplemental Figure S8. Scatterplots for replicates of transcriptome data.

Supplemental Table S1. Statistical phenotypic analysis results of the *cle* single, double, and triple mutants.

Supplemental Table S2. Primers used for genotyping.

Supplemental Table S3. Primers used for *DN-CLE* transgenic constructs in this work.

Supplemental Table S4. Primers used for quantitative real-time PCR analysis.

Supplemental Table S5. Primers used for in situ constructs in this work.

Supplemental Data Set S1. List of 578 genes down-regulated and 1,133 genes up-regulated in *DN-CLE19-23* transcriptomic analysis in this study.

Supplemental Data Set S2. List of 1,809 genes down-regulated and 379 genes up-regulated in *CLE19-OX-S* transcriptomic analysis in this study.

Supplemental Data Set S3. List of 742 genes both up-regulated in *DN-CLE19-23* and down-regulated in *CLE19-OX-S* transcriptomic data.

Supplemental Data Set S4. List of 52 genes both down-regulated in *DN-CLE19-23* and up-regulated in *CLE19-OX-S* transcriptomic data.

Supplemental Data Set S5. List of overlap genes differentially expressed in both *DN-CLE19-23* and *CLE19-OX-S* transcription data and the microarray-based transcriptomic data of the *ams* stage 4 to 7 anthers and 404 RNA-seq-based transcriptomic data of *ams* buds.

ACKNOWLEDGMENTS

We thank the Salk Institute Genomic Analysis Laboratory and the Ohio State University Arabidopsis Biological Resource Center for providing the sequence-indexed Arabidopsis T-DNA insertion mutants.

Received March 30, 2017; accepted September 12, 2017; published September 15, 2017.

LITERATURE CITED

Albrecht C, Russinova E, Hecht V, Baaijens E, de Vries S (2005) The *Arabidopsis thaliana* SOMATIC EMBRYOGENESIS RECEPTOR-LIKE KINASES1 and 2 control male sporogenesis. Plant Cell **17:** 3337–3349

Alexander MP (1969) Differential staining of aborted and nonaborted pollen. Stain Technol **44:** 117–122

Al-Refu K, Edward S, Ingham E, Goodfield M (2009) Alterations in the basement membrane zone in cutaneous lupus erythematosus (CLE) as demonstrated by immunohistochemistry. Arch Dermatol Res **301:** 47

Ariizumi T, Toriyama K (2011) Genetic regulation of sporopollenin synthesis and pollen exine development. Annu Rev Plant Biol **62:** 437–460

Bedinger PA, Hardeman KJ, Loukides CA (1994) Travelling in style: the cell biology of pollen. Trends Cell Biol **4:** 132–138

Blackmore S, Wortley AH, Skvarla JJ, Rowley JR (2007) Pollen wall development in flowering plants. New Phytol **174:** 483–498

Canales C, Bhatt AM, Scott R, Dickinson H (2002) EXS, a putative LRR receptor kinase, regulates male germline cell number and tapetal identity and promotes seed development in *Arabidopsis*. Curr Biol **12:** 1718–1727

Casamitjana-Martínez E, Hofhuis HF, Xu J, Liu CM, Heidstra R, Scheres B (2003) Root-specific CLE19 overexpression and the sol1/2 suppressors implicate a CLV-like pathway in the control of Arabidopsis root meristem maintenance. Curr Biol **13:** 1435–1441

Chang F, Wang Y, Wang S, Ma H (2011) Molecular control of microsporogenesis in Arabidopsis. Curr Opin Plant Biol **14:** 66–73

Clough SJ, Bent AF (1998) Floral dip: a simplified method for Agrobacterium-mediated transformation of *Arabidopsis thaliana*. Plant J **16:** 735–743

Cock JM, McCormick S (2001) A large family of genes that share homology with *CLAVATA3*. Plant Physiol **126:** 939–942

Colcombet J, Boisson-Dernier A, Ros-Palau R, Vera CE, Schroeder JI (2005) *Arabidopsis* SOMATIC EMBRYOGENESIS RECEPTOR KINASES1 and 2 are essential for tapetum development and microspore maturation. Plant Cell **17:** 3350–3361

Cui J, You C, Zhu E, Huang Q, Ma H, Chang F (2016) Feedback regulation of DYT1 by interactions with downstream bHLH factors promotes DYT1 nuclear localization and anther development. Plant Cell **28:** 1078–1093

DeYoung BJ, Bickle KL, Schrage KJ, Muskett P, Patel K, Clark SE (2006) The CLAVATA1-related BAM1, BAM2 and BAM3 receptor kinase-like proteins are required for meristem function in *Arabidopsis*. Plant J **45:** 1–16

Edlund AF, Swanson R, Preuss D (2004) Pollen and stigma structure and function: the role of diversity in pollination. Plant Cell (Suppl) **16:** S84–S97

Feng B, Lu D, Ma X, Peng Y, Sun Y, Ning G, Ma H (2012) Regulation of the Arabidopsis anther transcriptome by DYT1 for pollen development. Plant J **72:** 612–624

Ferguson AC, Pearce S, Band LR, Yang C, Ferjentsikova I, King J, Yuan Z, Zhang D, Wilson ZA (2017) Biphasic regulation of the transcription factor ABORTED MICROSPORES (AMS) is essential for tapetum and pollen development in Arabidopsis. New Phytol **213:** 778–790

Fiers M, Golemiec E, Xu J, van der Geest L, Heidstra R, Stiekema W, Liu CM (2005) The 14-amino acid CLV3, CLE19, and CLE40 peptides trigger consumption of the root meristem in *Arabidopsis* through a *CLAVATA2*-dependent pathway. Plant Cell **17:** 2542–2553

Fiers M, Hause G, Boutilier K, Casamitjana-Martinez E, Weijers D, Offringa R, van der Geest L, van Lookeren Campagne M, Liu CM (2004) Mis-expression of the *CLV3/ESR*-like gene *CLE19* in *Arabidopsis* leads to a consumption of root meristem. Gene **327:** 37–49

Fiume E, Fletcher JC (2012) Regulation of *Arabidopsis* embryo and endosperm development by the polypeptide signaling molecule CLE8. Plant Cell **24:** 1000–1012

Fletcher JC, Brand U, Running MP, Simon R, Meyerowitz EM (1999) Signaling of cell fate decisions by CLAVATA3 in Arabidopsis shoot meristems. Science **283:** 1911–1914

Ge X, Chang F, Ma H (2010) Signaling and transcriptional control of reproductive development in *Arabidopsis*. Curr Biol **20:** R988–R997

Goldberg RB, Beals TP, Sanders PM (1993) Anther development: basic principles and practical applications. Plant Cell **5:** 1217–1229

Gu JN, Zhu J, Yu Y, Teng XD, Lou Y, Xu XF, Liu JL, Yang ZN (2014) DYT1 directly regulates the expression of *TDF1* for tapetum development and pollen wall formation in Arabidopsis. Plant J **80:** 1005–1013

Guilford WJ, Schneider DM, Labovitz J, Opella SJ (1988) High resolution solid state C NMR spectroscopy of sporopollenins from different plant taxa. Plant Physiol **86:** 134–136

Honys D, Twell D (2004) Transcriptome analysis of haploid male gametophyte development in *Arabidopsis*. Genome Biol **5:** R85

Hord CL, Chen C, Deyoung BJ, Clark SE, Ma H (2006) The BAM1/BAM2 receptor-like kinases are important regulators of *Arabidopsis* early anther development. Plant Cell **18:** 1667–1680

Hord CL, Sun YJ, Pillitteri LJ, Torii KU, Wang H, Zhang S, Ma H (2008) Regulation of *Arabidopsis* early anther development by the mitogen-activated protein kinases, MPK3 and MPK6, and the ERECTA and related receptor-like kinases. Mol Plant **1:** 645–658

Huang J, Zhang T, Linstroth L, Tillman Z, Otegui MS, Owen HA, Zhao D (2016) Control of anther cell differentiation by the small protein ligand and TPD1 and its receptor EMS1 in *Arabidopsis*. PLoS Genet **12:** e1006147

Ito T, Nagata N, Yoshiba Y, Ohme-Takagi M, Ma H, Shinozaki K (2007) *Arabidopsis* MALE STERILITY1 encodes a PHD-type transcription factor and regulates pollen and tapetum development. Plant Cell **19:** 3549–3562

Jia G, Liu X, Owen HA, Zhao D (2008) Signaling of cell fate determination by the TPD1 small protein and EMS1 receptor kinase. Proc Natl Acad Sci USA **105:** 2220–2225

Jin Y, Yang H, Wei Z, Ma H, Ge X (2013) Rice male development under drought stress: phenotypic changes and stage-dependent transcriptomic reprogramming. Mol Plant **6:** 1630–1645

Jun J, Fiume E, Roeder AH, Meng L, Sharma VK, Osmont KS, Baker C, Ha CM, Meyerowitz EM, Feldman LJ, et al (2010) Comprehensive analysis of *CLE* polypeptide signaling gene expression and overexpression activity in Arabidopsis. Plant Physiol **154:** 1721–1736

Karimi M, Inzé D, Depicker A (2002) GATEWAY vectors for Agrobacterium-mediated plant transformation. Trends Plant Sci **7:** 193–195

Kim SS, Douglas CJ (2013) Sporopollenin monomer biosynthesis in Arabidopsis. J Plant Biol **56:** 1–6

Laux T, Mayer KF, Berger J, Jürgens G (1996) The *WUSCHEL* gene is required for shoot and floral meristem integrity in *Arabidopsis*. Development **122:** 87–96

Li H, Zhang D (2010) Biosynthesis of anther cuticle and pollen exine in rice. Plant Signal Behav **5:** 1121–1123

Li Z, Wang Y, Huang J, Ahsan N, Biener G, Paprocki J, Thelen JJ, Raicu V, Zhao D (2017) Two SERK receptor-like kinases interact with EMS1 to control anther cell fate determination. Plant Physiol **173:** 326–337

Ma H (2005) Molecular genetic analyses of microsporogenesis and microgametogenesis in flowering plants. Annu Rev Plant Biol **56:** 393–434

Ma X, Feng B, Ma H (2012) AMS-dependent and independent regulation of anther transcriptome and comparison with those affected by other Arabidopsis anther genes. BMC Plant Biol **12:** 23

Mariani C, Beuckeleer MD, Truettner J, Leemans J, Goldberg R (1990) Induction of male sterility in plants by a chimaeric ribonuclease gene. Nature **347:** 737–741

Mascarenhas JP (1975) The biochemistry of angiosperm pollen development. Bot Rev **41:** 259–314

Mayfield JA, Preuss D (2000) Rapid initiation of Arabidopsis pollination requires the oleosin-domain protein GRP17. Nat Cell Biol **2:** 128–130

Mizuno S, Osakabe Y, Maruyama K, Ito T, Osakabe K, Sato T, Shinozaki K, Yamaguchi-Shinozaki K (2007) Receptor-like protein kinase 2 (RPK 2) is a novel factor controlling anther development in *Arabidopsis thaliana*. Plant J **50:** 751–766

Ni J, Clark SE (2006) Evidence for functional conservation, sufficiency, and proteolytic processing of the CLAVATA3 CLE domain. Plant Physiol **140:** 726–733

Pacini E, Juniper BE (1979) The ultrastructure of pollen-grain development in the olive (*Olea europaea*). 2. Secretion by the tapetal cells. New Phytol **83:** 165–174

Phan HA, Iacuone S, Li SF, Parish RW (2011) The MYB80 transcription factor is required for pollen development and the regulation of tapetal programmed cell death in *Arabidopsis thaliana*. Plant Cell **23:** 2209–2224

Preuss D, Lemieux B, Yen G, Davis RW (1993) A conditional sterile mutation eliminates surface components from *Arabidopsis* pollen and disrupts cell signaling during fertilization. Genes Dev **7:** 974–985

Sanders PM, Bui AQ, Weterings K, Mcintire KN, Hsu YC, Pei YL, Mai TT, Beals TP, Goldberg RB (1999) Anther developmental defects in *Arabidopsis thaliana* male-sterile mutants. Plant Reprod **11:** 297–322

Scott RJ, Spielman M, Dickinson HG (2004) Stamen structure and function. Plant Cell (Suppl) **16:** S46–S60

Shpak ED, Lakeman MB, Torii KU (2003) Dominant-negative receptor uncovers redundancy in the *Arabidopsis* ERECTA leucine-rich repeat receptor-like kinase signaling pathway that regulates organ shape. Plant Cell **15:** 1095–1110

Song XF, Guo P, Ren SC, Xu TT, Liu CM (2013) Antagonistic peptide technology for functional dissection of *CLV3/ESR* genes in Arabidopsis. Plant Physiol **161:** 1076–1085

Song XF, Yu DL, Xu TT, Ren SC, Guo P, Liu CM (2012) Contributions of individual amino acid residues to the endogenous CLV3 function in shoot apical meristem maintenance in Arabidopsis. Mol Plant **5:** 515–523

Sorensen AM, Kröber S, Unte US, Huijser P, Dekker K, Saedler H (2003) The Arabidopsis *ABORTED MICROSPORES* (*AMS*) gene encodes a MYC class transcription factor. Plant J **33:** 413–423

Stahl Y, Simon R (2009) Is the Arabidopsis root niche protected by sequestration of the CLE40 signal by its putative receptor ACR4? Plant Signal Behav **4:** 634–635

Stieglitz H (1977) Role of β-1,3-glucanase in postmeiotic microspore release. Dev Biol **57:** 87–97

Strabala TJ, O'Donnell PJ, Smit AM, Ampomah-Dwamena C, Martin EJ, Netzler N, Nieuwenhuizen NJ, Quinn BD, Foote HC, Hudson KR (2006) Gain-of-function phenotypes of many *CLAVATA3/ESR* genes, including four new family members, correlate with tandem variations in the conserved CLAVATA3/ESR domain. Plant Physiol **140:** 1331–1344

Thom I, Grote M, Abraham-Peskir J, Wiermann R (1998) Electron and x-ray microscopic analyses of reaggregated materials obtained after fractionation of dissolved sporopollenin. Protoplasma **204:** 13–21

Torii KU, Mitsukawa N, Oosumi T, Matsuura Y, Yokoyama R, Whittier RF, Komeda Y (1996) The *Arabidopsis ERECTA* gene encodes a putative receptor protein kinase with extracellular leucine-rich repeats. Plant Cell **8:** 735–746

Wilson ZA, Morroll SM, Dawson J, Swarup R, Tighe PJ (2001) The Arabidopsis *MALE STERILITY1* (*MS1*) gene is a transcriptional regulator of male gametogenesis, with homology to the PHD-finger family of transcription factors. Plant J **28:** 27–39

Wilson ZA, Zhang DB (2009) From *Arabidopsis* to rice: pathways in pollen development. J Exp Bot **60:** 1479–1492

Xiong SX, Lu JY, Lou Y, Teng XD, Gu JN, Zhang C, Shi QS, Yang ZN, Zhu J (2016) The transcription factors MS188 and AMS form a complex to activate the expression of *CYP703A2* for sporopollenin biosynthesis in *Arabidopsis thaliana*. Plant J **88:** 936–946

Xu J, Ding Z, Vizcay-Barrena G, Shi J, Liang W, Yuan Z, Werck-Reichhart D, Schreiber L, Wilson ZA, Zhang D (2014) ABORTED MICROSPORES acts as a master regulator of pollen wall formation in *Arabidopsis*. Plant Cell **26:** 1544–1556

Xu J, Yang C, Yuan Z, Zhang D, Gondwe MY, Ding Z, Liang W, Zhang D, Wilson ZA (2010) The ABORTED MICROSPORES regulatory network is required for postmeiotic male reproductive development in *Arabidopsis thaliana*. Plant Cell **22:** 91–107

Xu TT, Ren SC, Song XF, Liu CM (2015) *CLE19* expressed in the embryo regulates both cotyledon establishment and endosperm development in Arabidopsis. J Exp Bot **66:** 5217–5227

Yang L, Qian X, Chen M, Fei Q, Meyers B, Liang W, Zhang D (2016) Regulatory role of a receptor-like kinase in specifying anther cell identity. Plant Physiol **171:** 2085–2100

Yang SL, Jiang L, Puah CS, Xie LF, Zhang XQ, Chen LQ, Yang WC, Ye D (2005) Overexpression of *TAPETUM DETERMINANT1* alters the cell fates in the Arabidopsis carpel and tapetum via genetic interaction with *EXCESS MICROSPOROCYTES1/EXTRA SPOROGENOUS CELLS*. Plant Physiol **139:** 186–191

Yang SL, Xie LF, Mao HZ, Puah CS, Yang WC, Jiang L, Sundaresan V, Ye D (2003) *Tapetum determinant1* is required for cell specialization in the *Arabidopsis* anther. Plant Cell **15:** 2792–2804

Ye Q, Zhu W, Li L, Zhang S, Yin Y, Ma H, Wang X (2010) Brassinosteroids control male fertility by regulating the expression of key genes involved in *Arabidopsis* anther and pollen development. Proc Natl Acad Sci USA **107:** 6100–6105

Zhang W, Sun Y, Timofejeva L, Chen C, Grossniklaus U, Ma H (2006) Regulation of Arabidopsis tapetum development and function by *DYSFUNCTIONAL TAPETUM1* (*DYT1*) encoding a putative bHLH transcription factor. Development **133:** 3085–3095

Zhao DZ, Wang GF, Speal B, Ma H (2002) The *excess microsporocytes1* gene encodes a putative leucine-rich repeat receptor protein kinase that

controls somatic and reproductive cell fates in the Arabidopsis anther. Genes Dev **16:** 2021–2031

Zhu E, You C, Wang S, Cui J, Niu B, Wang Y, Qi J, Ma H, Chang F (2015) The DYT1-interacting proteins bHLH010, bHLH089 and bHLH091 are redundantly required for *Arabidopsis* anther development and transcriptome. Plant J **83:** 976–990

Zhu J, Chen H, Li H, Gao JF, Jiang H, Wang C, Guan YF, Yang ZN (2008) *Defective in Tapetal development and function 1* is essential for anther development and tapetal function for microspore maturation in Arabidopsis. Plant J **55:** 266–277

Zhu J, Lou Y, Xu X, Yang ZN (2011) A genetic pathway for tapetum development and function in *Arabidopsis*. J Integr Plant Biol **53:** 892–900

Zinkl GM, Zwiebel BI, Grier DG, Preuss D (1999) Pollen-stigma adhesion in *Arabidopsis*: a species-specific interaction mediated by lipophilic molecules in the pollen exine. Development **126:** 5431–5440